Chapter 1

Theory of neutrino physics

Just give a short overview of the historical context, but mainly focusing on the actual description of the neutrino theory, mostly stating the fact rather than giving a large background

I should discuss everything that is even briefly mentioned in the neutrino magnetic moment theory section.

- Dirac vs Majorana neutrinos
- Neutrino masses
- Neutrino interactions with electrons and nuclei
- Neutrino oscillations and their implications

The story:

1. Brief history up to neutrinos being in the SM
2. Description of neutrinos in the SM
3. Interactions of neutrinos and their detection
4. Production of neutrinos
5. Solar and atmospheric neutrino anomalies and neutrino oscillations
6. Detail of neutrino oscillations for three flavours
7. Current state of neutrino oscillation measurements
8. Mass ordering, octant, delta CP
9. Neutrino masses - generation and measurements

10. Dirac V Majorana neutrinos

Neutrinos were first introduced by Pauli [1, 2] as very light electrically neutral particles with half-spin and a possible magnetic moment [3]. They were a crucial part of Enrico Fermi's successful theory of β decays [4, 5], which solidified their importance in particle physics even before their first experimental detection. Fermi's theory developed into the Standard Model (SM) of particle physics [6–8], which in its current form contains three generations of fermions. Each generations contains two quarks, one charged lepton and an associated neutrino with no mass or magnetic moment.

SM is mathematically described by a Lagrangian, in which neutrinos are expressed as two-component left-handed chiral fields $\nu_{\alpha L}$, where $\alpha = e, \mu, \tau$ denotes the three neutrino generations, also called flavours [9–11]. Neutrinos form weak isospin doublets with their associated left handed charged lepton fields α_L. Unlike for the charged leptons, there is no right handed neutrino singlet in the SM. This means that neutrinos cannot obtain a (Dirac) mass term, since the mass terms for fermions arise from the Higgs mechanism [12–14] via the Yukawa coupling of the fermion and the Higgs fields [15], which requires a combination of left-handed and right-handed fields [16].

The interaction terms for neutrinos can be separated into two components defined by the vector gauge field they interact with. They are describing the Charged current (CC) and the Neutral Current (NC) interactions, based on whether they interact with the W_μ or Z_μ fields, which describe the $W^\pm$ or Z^0 weak boson respectively. Neglecting the non-neutrino components, the neutrinos interaction terms are [16]

$$\mathcal{L}^{\text{SM}}_{\text{CC}} = -\frac{g_w}{2\sqrt{2}} j^\mu_W W_\mu + \text{h.c.}, \quad \text{and} \quad \mathcal{L}^{\text{SM}}_{\text{NC}} = -\frac{g_w}{2\cos(\theta_W)} j^\mu_Z Z_\mu. \tag{1.1}$$

Here g_w is the weak coupling constant, θ_W is the Weinberg angle and j^μ_W and j^μ_Z are the weak currents expressed as

$$j^\mu_W = 2 \sum_{\alpha=e,\mu,\tau} \overline{\nu}_{\alpha L} \gamma^\mu \alpha_L, \tag{1.2}$$

$$j^\mu_Z = 2 \sum_{\alpha=e,\mu,\tau} g^\nu_L \overline{\nu}_{\alpha L} \gamma^\mu \nu_{\alpha L}. \tag{1.3}$$

$\gamma^\mu, \mu = 0, 1, 2, 3$, are the four Dirac gamma matrices and g^ν_L is the coupling term,

which for neutrinos $g_L^\nu = +1/2$.

The two terms of the interaction Lagrangian from Eq. 1.1 describe the possible neutrino interaction vertices, shown in Fig. 1.1. These diagrams show the CC and NC interaction of neutrinos and antineutrinos and, in case of the CC diagram, can also be flipped around the vertical axis to show the production of neutrinos from the weak interaction (or decays) of leptons. They can also be rotated $90°$ to show annihilation, or production, of the neutrino-lepton (for CC), or neutrino-antineutrino (for NC) pairs.

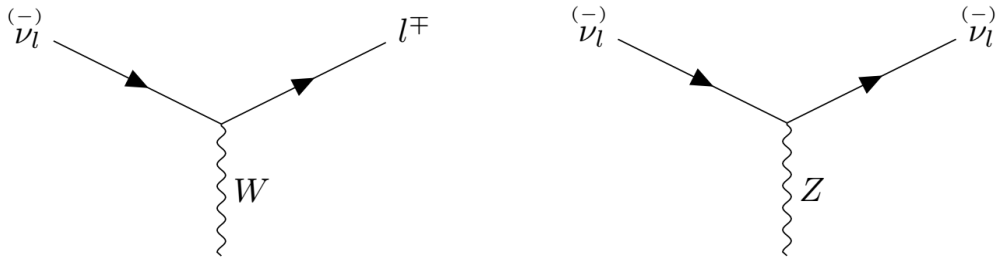

Figure 1.1: Neutrino interaction vertices in the SM via the weak charged currents (left) and the neutral currents (right).

1.1 Neutrino Production

Some of the most common neutrino and antineutrino production channels include nucleon transitions via CC weak interactions. Specifically, the transition of a neutron into a proton, either as a decay of a free neutron, or as a β^- decay for neutrons bound in a nucleus, produces an electron and an electron antineutrino:

$$n \rightarrow p + e^- + \overline{\nu}_e. \tag{1.4}$$

The shape of the electron spectrum from a β^- decay was the reason Pauli proposed the existence of the neutrino [1]. Additionally, this channel is an abundant source of $\overline{\nu}_e$ from nuclear reactors, which were the first artificial sources of neutrinos, increasing the neutrino flux by about 100 million compared to the naturally occurring sources, enabling the first ever detection of a neutrino [17–19].

Similarly, the production of an electron neutrino via the transition of a proton

into a neutron can occur inside the nucleus either as the β^+ decay:

$$p \rightarrow n + e^+ + \nu_e, \tag{1.5}$$

or via the electron capture:

$$p + e^- \rightarrow n + \nu_e. \tag{1.6}$$

This channel occurs in stars and in the first phase of supernovae [16]. However, most supernovae neutrinos are created via a thermal pair production via NC interaction

$$e^- + e^+ \rightarrow \nu_\alpha + \overline{\nu}_\alpha \tag{1.7}$$

producing neutrinos and antineutrinos of all flavours. The neutrino pair production via the decay of Z^0 was studied in great detail [20], since the magnitude of the decay width depends on the number of light active neutrino flavours. The current best fit is $N_\nu = 2.984$ [21].

An abundant source of ν_μ and $\overline{\nu}_\mu$ is the decay of pions and muons

$$p + X \rightarrow \pi^\pm \rightarrow \mu^\pm + \nu_\mu \left(\overline{\nu}_\mu\right) \tag{1.8}$$

$$\mu^\pm \rightarrow e^\pm + \nu_\mu \left(\overline{\nu}_\mu\right) + \nu_e \left(\overline{\nu}_e\right), \tag{1.9}$$

which naturally occurs in Earth's atmosphere from the interaction of cosmic ray protons. Notice, that if all muons decay by the time they reach Earth's surface, the ratio of $\nu_\mu : \nu_e$ should be exactly 2:1. This processed is also used in the modern accelerator-based source of neutrinos, which accelerate protons to the desired energies, shoot them onto a fixed target, and focus the resulting hadrons to achieve a highly pure and precise source of ν_μ or $\overline{\nu}_\mu$ [22, 23]. Similarly, decays of heavier hadrons, such as kaons and charmed particles, also produce neutrinos, including ν_τ and $\overline{\nu}_\tau$ [24, 25].

1.2 Neutrino Interactions

The interaction of neutrinos can either be categorized based on the target, which is generally either electron or a nucleus, or on the neutrino energy. Neutrino-electron interactions either occur via elastic scattering, which has the same neutrino and an

electron in the final state, or via the inverse muon (or tau) decay, which contains a muon (or tau) in the final state. Both of these interactions are purely governed by Quantum Electro Dynamics (QED) and are theoretically very well understood, using their measurements to provide constraints on the parameters within the QED theory. While the neutrino-on-electron elastic scattering does not have a threshold energy and can occur for any neutrinos, the inverse muon decay has a threshold energy of $10.92\,\mathrm{GeV}$, and the inverse tau decay $> 3\,\mathrm{TeV}$ [16, 26].

The interaction of neutrinos on a nucleus is more complicated, due to contributions from possible nuclear effects and the non-trivial nature of the individual nucleons. At low neutrino energies, the only currently detectable

CEvENS [27]

For low energies neutrinos typically interact with the entire nucleus, either via CEvENS, or either via various nuclear models. At higher energies neutrinos start to probe the individual nucleons. At higher energies still, the produced nucleons can get excited and at higher energies still neutrinos start to probe inside the nucleons themselves.

For neutrinos interacting on the nuclei, we distinguish between different types of interactions based on what happens to the nucleus. If it's an interaction with a single proton or neutron, we call this Quasi Elastic (QE) interaction. If this proton gets excited into a Δ resonance (which then generally decays into a π), we call this Resonant production, if neutrino penetrates through the nucleon and interacts directly with a quark inside it, we call this Deep Inelastic Scattering (DIS) interaction. This is shown on Fig. 1.2. There can be additional subtypes due to nuclear effects, namely the 2p2h interaction TO DO: *Find a reference for the 2p2h* also called Meson Exchange Current (MEC), or possible Final State Interaction (FSI).

Inversely, the detection of neutrinos is usually done by reverting the above mentioned processes. The discussion of neutrino interactions is in [29]

For example for the $\overline{\nu}_e$ we can use the so-called inverse beta decay

$$\overline{\nu}_e + p \rightarrow n + e^+ \tag{1.10}$$

was used for the first detection of neutrinos by Cowan and Reines [17, 18]. This is currently used in the reactor neutrino experiments COMMENT: *Should I mention*

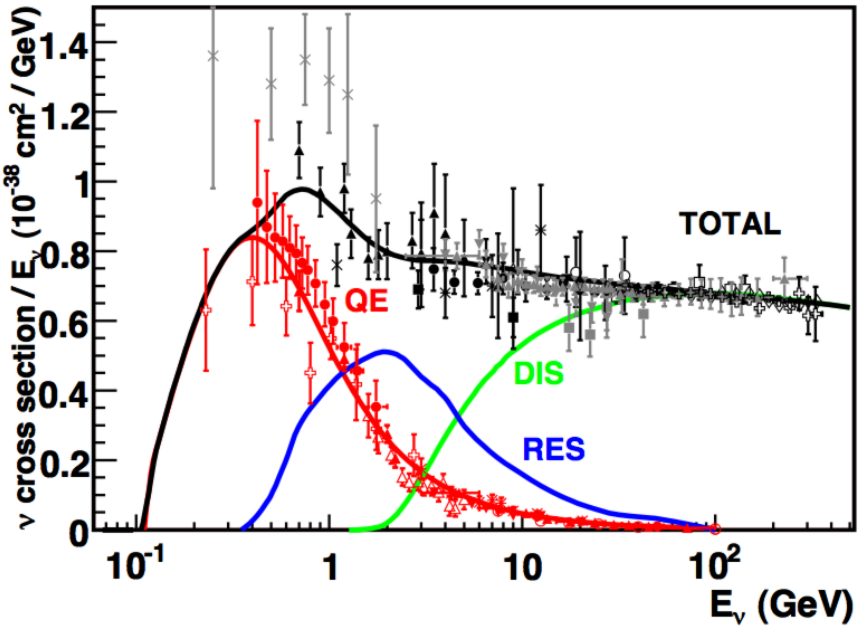

Figure 1.2: Neutrino CC cross sections based on the interaction types. Figure from [28] compares the measured data [29] and the prediction [30]

some reactor experiments here?

[16] nu-on-e is for example used for the detection of solar neutrinos in the Kamiokande experiments Nu-on-e is mainly sensitive to electron neutrinos, whose cross section is about 6 times larger than for the muon/tau neutrinos.

The first electron neutrino detection was by the Homestake neutrino experiment detecting solar neutrinos [31] $\nu_e + n \rightarrow p + e^-$

Leon Lederman, Jack Steinberger and others joined Schwartz and using a spark chamber detector in 1962 observed [32] for the first time the muon neutrino ν_μ. Atmospheric neutrinos were first observed by the Kolar Gold Field Mine in South India [33, 34] and in the East Rand Proprietary Gold Mine in South Africa [35].

After this result it was only a matter of time, before the third neutrino, the tau neutrino (ν_τ) was discovered. Evidence for that were shown in 2000 from the DONUT Collaboration at Fermilab [24].

I think I should mention here the basic neutrino interactions and their corresponding cross section. For neutrino on nucleons, the total cross section per neutrino energy is around $0.7 \times 10^{-38}\,\mathrm{cm}^2\mathrm{GeV}^{-1}$ for neutrinos and half that for antineutrinos. For neutrino on electron interactions, the total cross section per neutrino energy is more similar to $10^-41 - 10^{-42}\,\mathrm{cm}^2\mathrm{GeV}^{-1}$.

The main neutrino interactions are

$$\nu_l + n \rightarrow p + l^- \tag{1.11}$$

$$\overline{\nu}_l + p \rightarrow n + l^+ \tag{1.12}$$

$$\nu_l + N \rightarrow \nu_l + N \tag{1.13}$$

$$\overline{\nu}_l + N \rightarrow \overline{\nu}_l + N \tag{1.14}$$

Problems of the SM

TO DO: *Describe neutrino interactions, CC, NC elastic. QE, Res., DIS. Also nuclear effects - MEC, FSI,...*

1.3 Neutrino Oscillation

Neutrino oscillate and therefore have mass. Describe neutrino oscillations and the current status of their measurements. Maybe also when they were discovered and how?

[Master's] Several experimental indications for neutrino oscillations were found shortly after its theoretical predictions. Already in 1968 their Homestake Solar Neutrino Observatory saw a solar neutrino flux less than 3 Solar Neutrino Units (SNU = one interaction per 10^{36} target atoms s^{-1}), well below the solar model prediction of the time [31]. This discrepancy became the *"solar neutrino problem"*, which is in line with neutrino oscillations, but no direct implications could have been drawn since it might have been caused by a lack of understanding of nuclear physics, astrophysics of the Sun, or particle physics of the neutrino[22]. Kamiokande experiment, which confirmed the results from Homestake [36].

The Solar neutrino anomaly was also resolved, when the Sudbury Neutrino Observatory (SNO) provided $> 5\sigma$ evidence for solar ν_e oscillations in 2002, independent on the solar model [37]. While other solar neutrino experiments measured solar ν_e only via the charged current (CC) interactions

$$\nu_e + n \rightarrow p + e^- \qquad (CC), \tag{1.15}$$

SNO had an ability to also detect neutrinos via the neutral current (NC) interaction

$$\nu + X \rightarrow \nu + X' \qquad (NC), \tag{1.16}$$

which are equally sensitive to all active neutrino flavours and their rate is therefore unaffected by standard neutrino oscillations. SNO could compare CC and NC event rates and conclude that ν_e from the Sun oscillate into other neutrino flavours along the way [37].

Measuring atmospheric neutrinos brought about another neutrino conundrum, the *Atmospheric neutrino anomaly*. It came from the disagreement between experiments such as NUSEX[38] and Fréjus[39], which used iron calorimeters detectors, and experiments IMP[40] and Kamiokande[41], which used water Cherenkov detectors. All of these experiments were looking for a deficit of ν_μ, or an excess of ν_e, compared to prediction. While the first two experiments saw a good agreement between experimental results and predictions, the latter two did not and suggested the possibility of neutrino oscillations, which could explain their disagreement. Solution to the Atmospheric neutrino anomaly came in 1998, when the Super-Kamiokande (SK) experiment showed for the first time the experimental evidence for neutrino oscillations [42]. SK has however also disfavoured the two neutrino hypothesis, with regards to the existence of an additional neutrino flavour.

The idea that neutrinos can oscillate between the individual flavours originates [43, 44] from the $K^0 \leftrightarrow \overline{K^0}$ oscillations, which was adapted to neutrinos [45, 46] by considering that the weak interaction neutrino eigenstates ν_α produced in CC weak interaction are not identical to the mass neutrino eigenstates ν_k and are related by

$$|\nu_\alpha\rangle = \sum_k U^*_{\alpha k} |\nu_k\rangle \,. \tag{1.17}$$

Here U is a unitary matrix now know by the authors of neutrino oscillations as Pontecorvo Maki Nakagawa Sakata (PMNS) matrix [16, 47].

The massive neutrino states $|\nu_i\rangle$ are eigenstates of the hamiltonian

$$\mathcal{H} |\nu_k\rangle = E_i |\nu_k\rangle \,, \tag{1.18}$$

where

$$E_k = \sqrt{\overrightarrow{p}^2 + m_k^2} \tag{1.19}$$

and since neutrinos are generally ultrarelativistic, we can approximate their energy as

$$E_k \xrightarrow{m^2 \ll p^2 \approx E^2} E + \frac{m_k^2}{E}. \tag{1.20}$$

From the Schrodinger equation

$$i\frac{d}{dt}\left|\nu_k\left(t\right)\right\rangle = \mathcal{H}\left|\nu_k\left(t\right)\right\rangle \tag{1.21}$$

we get that the massive neutrino states evolve as plane waves

$$\left|\nu_k\left(t\right)\right\rangle = e^{-iE_k t}\left|\nu_k\right\rangle. \tag{1.22}$$

Also thanks to the unitarity of the mixing matrix we get

$$\left|\nu_k\right\rangle = \sum_\alpha U_{\alpha k}\left|\nu_\alpha\right\rangle \tag{1.23}$$

and therefore

$$\left|\nu_\alpha\left(t\right)\right\rangle = \sum_\beta \sum_k U_{\alpha k}^* U_{\beta k} e^{-iE_k t}\left|\nu_\beta\right\rangle. \tag{1.24}$$

Since both the massive neutrino states and the flavour neutrino states are built in an orthogonal basis $\langle\nu_k|\nu_j\rangle = \delta_{kj}$ and $\langle\nu_\alpha|\nu_\beta\rangle = \delta_{\alpha\beta}$ we can write the amplitude of the $\nu_\alpha \to \nu_\beta$ transitions as

$$A_{\nu_\alpha \to \nu_\beta}\left(t\right) \equiv \langle\nu_\beta|\nu_\alpha\left(t\right)\rangle = \sum_k U_{\alpha k}^* U_{\beta k} e^{-iE_k t} \tag{1.25}$$

Given the ultrarelativistic approximation in Eq. 1.20, assuming the time t is equivalent to the distance L, which is easier to measure in an experiment, we get the prob-

ability that ν_α oscillates into ν_β over the course of distance L with an energy E is

$$P_{\nu_\alpha \to \nu_\beta}(L) = \left| A_{\nu_\alpha \to \nu_\beta}(t) \right|^2 = \sum_{k,j} U^*_{\alpha k} U_{\beta j} U_{\alpha j} U^*_{\beta j} e^{-i(E_k - E_j)L} \tag{1.26}$$

$$P_{\nu_\alpha \to \nu_\beta}(L) = \sum_{k,j} U^*_{\alpha k} U_{\beta j} U_{\alpha j} U^*_{\beta j} e^{-i\frac{\Delta m^2_{kj} L}{2E}}. \tag{1.27}$$

We defined the so-called neutrino mass splitting as

$$\Delta m^2_{kj} \equiv m^2_k - m^2_j. \tag{1.28}$$

The PMNS matrix for mixing of three massive (Dirac) neutrinos with three neutrino flavours can be parametrized with four independent parameters: three mixing angles (θ_{12}, θ_{13}, θ_{23}) and a δ_{CP} phase, which, if different from 0 or π, implies the Charge conjugation - Parity (CP) symmetry violation, and the other two are α and β, so called Majorana phases, which are non zero only if neutrinos are Majorana (neutrinos and antineutrinos are described by just one field, i.e. neutrinos are the same particle as antineutrinos). Majorana phases play no role in neutrino oscillations, so they are usually left out in the description [48]. The PMNS matrix in this case can be parametrized as

$$U = \begin{pmatrix} U_{e1} & U_{e2} & U_{e3} \\ U_{\mu 1} & U_{\mu 2} & U_{\mu 3} \\ U_{\tau 1} & U_{\tau 2} & U_{\tau 3} \end{pmatrix} =$$

$$= \begin{pmatrix} 1 & 0 & 0 \\ 0 & c_{23} & s_{23} \\ 0 & -s_{23} & c_{23} \end{pmatrix} \begin{pmatrix} c_{13} & 0 & s_{13} e^{-i\delta} \\ 0 & 1 & 0 \\ -s_{13} e^{i\delta} & 0 & c_{13} \end{pmatrix} \begin{pmatrix} c_{12} & s_{12} & 0 \\ -s_{12} & c_{12} & 0 \\ 0 & 0 & 1 \end{pmatrix} \begin{pmatrix} 1 & 0 & 0 \\ 0 & e^{i\alpha} & 0 \\ 0 & 0 & e^{i\beta} \end{pmatrix}, \tag{1.29}$$

where $c_{ij} \equiv \cos\theta_{ij}$ and $s_{ij} \equiv \sin\theta_{ij}$.

Other than the PMNS matrix, neutrino oscillations depend on the mass squared differences (eq.1.28). In case of 3 neutrinos, those are Δm^2_{21} and Δm^2_{31}. Δm^2_{21} mainly drives oscillations of solar neutrinos and is therefore often denoted as $\Delta m^2_\odot$ or Δm^2_{sol}, while Δm^2_{31} drives oscillations on the scale for atmospheric neutrinos and is often written as Δm^2_{atm} [47]. There can only be two independent mass squared differences

for oscillation of three neutrinos, since

$$\Delta m^2_{21} + \Delta m^2_{32} + \Delta m^2_{13} = 0. \tag{1.30}$$

1.3.1 The Matter Effect

Possible explanation of the Solar neutrino problem was proposed in 1978 by L. Wolfenstein, who considered the effect of matter on neutrino oscillations [49]. His modification of neutrino oscillations when passing through matter arises from the coherent forward scattering of electron neutrinos, as a result of their charged current (CC) interaction with electrons, which are abundant in matter, as opposed to other lepton flavours, muons and tauons, resulting in an imbalance between ν_e and ν_μ/ν_τ. This manifests as an effective potential, which depends on the density and composition of the matter [49]. This idea was later further developed for neutrinos passing through the Sun by Mikheyev and Smirnov in 1985 [50][47] and we now call this effect the Mikheyev-Smirnov-Wolfenstein (MSW) effect.

To showcase this effect we consider only two neutrino flavours, ν_e and ν_X, where X denotes a combination of all other non-electron flavours. Vacuum oscillations are in this two-neutrino approximation driven by a single mass splitting Δm^2 and the corresponding PMNS matrix is a rotational matrix parametrized by one angle θ:

$$U = \begin{pmatrix} \cos\theta & \sin\theta \\ -\sin\theta & \cos\theta \end{pmatrix}. \tag{1.31}$$

The MSW effect can be described as the presence of an Effective Potential [51]

$$V = \pm\sqrt{2} G_F N_e = \pm 3.8 \times 10^{-14} \left(\frac{\rho}{\text{g cm}^{-3}}\right) \left(\frac{Y_e}{0.5}\right) \text{eV}, \tag{1.32}$$

where G_F is the Fermi coupling constant, N_e is the electron density, Y_e is the electron number per nucleon and plus or minus sign is for neutrinos or antineutrinos respectively.

This potential can be seen as having the effect of modifying the Δm^2 and θ of the

neutrino oscillations: [51]

$$\sin^2 2\theta_m = \frac{\sin^2 2\theta}{\sin^2 2\theta + (\cos 2\theta \mp \xi)^2} \tag{1.33}$$

$$\left(\Delta m^2\right)_{\mathit{eff}} = \Delta m^2 \times \sqrt{\sin^2 2\Theta + (\cos 2\theta \mp \xi)^2}, \tag{1.34}$$

where

$$\xi = \frac{2\sqrt{2} G_F N_e}{\Delta m^2}. \tag{1.35}$$

Need to mention the importance of the δ_{CP} measurements, maybe even the Sakharov conditions... Also why do we care about the Δm^2 or the octants and what are those... Maybe cite the Snowmass report and the PDG.

1.4 Neutrino Mass

Experiments for their values? Theoretical predictions for how they obtained them

Theories of neutrino mass generation

[Fundamentals of neutrinos physics and astrophysics] The only extension of the SM that is needed is the introduction of right-handed components $\nu_{\alpha R}$ of the neutrino fields. Such a model is sometimes called the *minimally extended Standard Model*. The right handed neutrino fields are fundamentally different from the other elementary fermion fields because they are invariant under the symmetries of the SM: they are **singlets** of $\mathrm{SU}(3)_C \times \mathrm{SU}(2)_L$ and have hypercharge $Y = 0$. The right handed neutrino fields are called sterile [883] because they do not participate in weak interactions and their only interaction is gravitational. their right handedness is not required though! could also be left handed but have to be singlets and therefore sterile!

In the minimally extended standard model with three right handed neutrino fields, the SM Higgs-lepton Yukawa Lagrangian is extended by adding a lepton term with the same structure as the second term on the right handed side, which generates the masses of up-type quarks

$$\mathcal{L}_Y = -\sum_{\alpha,\beta=e,\mu,\tau} Y'^{l}_{\alpha\beta} \overline{L}_{\alpha L} \Phi l'_{\beta R} - \sum_{\alpha,\beta=e,\mu,\tau} Y'^{\nu}_{\alpha\beta} \overline{L}_{\alpha L} \tilde{\Phi} \nu'_{\beta R} + \mathrm{h.c.}, \tag{1.36}$$

where Y'^{ν} is a new matrix of Yukawa couplings.

Using the unitary gauge we can diagonalize the Yukawa couplings we obtain

$$\mathcal{L}_Y = -\sum_{\alpha=e,\mu,\tau} \frac{y_\alpha^l v}{\sqrt{2}} \bar{l}_\alpha l_\alpha - \sum_{k=1}^{N} \frac{y_k^\nu v}{\sqrt{2}} \overline{\nu}_k \nu_k - \sum_{\alpha=e,\mu,\tau} \frac{y_\alpha^l}{\sqrt{2}} \bar{l}_\alpha l_\alpha H - \sum_{k=1}^{N} \frac{y_k^\nu}{\sqrt{2}} \overline{\nu}_k \nu_k H \quad (1.37)$$

Therefore the neutrino masses are given by

$$m_k = \frac{y_k^\nu v}{\sqrt{2}} \quad (k = 1, ..., N)\,, \quad (1.38)$$

and massive Dirac neutrinos couple to the Higgs field through the last term. Note that the neutrinos masses are proportional to the Higgs VEV v, as the masses of charged leptons and quarks. However, it is known that the masses of neutrinos are much smaller than those of charged leptons and quarks, but there is no explanations here of the very small values of the eigenvalues Y_k^ν of the Higgs-neutrino Yukawa coupling matrix that are needed. The lagrangian defined this way does not conserve the lepton flavour number, which leads to neutrino oscillations. The Dirac character of massive neutrinos is closely related to the invariance of the total Lagrangian under the global U(1) gauge transformations.

The sterile neutrino fields do not participate in weak interaction with both their left and right components, but can couple with the ordinary neutrinos through the mass therm, generating a complicated mixing between active and sterile degrees of freedom.Since at present there is no indication of the existence of such additional sterile Dirac neutrino fields, ockham's razor suggests to ignore them...

1.4.1 Majorana neutrinos

[Fundamentals of neutrinos physics and astrophysics,p.190] If the neutrino is massless, since the left handed chiral component of the neutrino field obeys the Weyl equation in both the Dirac and Majorana descriptions and the right handed chiral component is irrelevant for neutrino interactions, the Dirac and Majorana theories are physically equivalent. From this it is clear that in practice one can distinguish a Dirac from a Majorana neutrino only by measuring some effect due to the neutrino mass. Moreover, the mass effect must not be of kinematical nature, because the kinematical effects of Dirac and Majorana masses are the same. For example, the Dirac

and Majorana nature of neutrinos cannot be revealed through neutrino oscillations! The most promising way to find if neutrinos are Majorana particles is the search for neutrinoless double beta decay.

[OverviewOfNeutrinoPhysicsPheno2024.pdf] In contrast, the Majorana phases do not enter the flavour neutrino oscillation probabilities [22, 85], but contribute to the $\beta\beta_{0\nu}$ decay rate

Chapter 2

Muon Neutrino Magnetic Moment Measurement

2.1 Theory of neutrino magnetic moment

TO DO: *Re-read the three main theory papers and double check the theoretical overview*

In the Standard Model (SM), neutrinos are massless and electrically neutral particles. However, even in the SM neutrinos can have electromagnetic interaction through loop diagrams involving the charged leptons and the W boson. These interactions are described by the neutrino charge radius, described in section 2.1.2 [**?**].

To include neutrino masses required by neutrino oscillations, we must go Beyond the Standard Model (BSM), where neutrinos can acquire other electromagnetic properties [**?**]. In the most general case, considering interactions with a single photon as shown on Fig. 2.1, neutrino electromagnetic interactions can be described by an *effective* interaction Hamiltonian [**?**]

$$\mathcal{H}_{em}^{(\nu)}(x) = \sum_{k,j=1}^{N} \overline{\nu}_k(x)\, \Lambda_\mu^{kj} \nu_j(x)\, A^\mu(x)\,. \tag{2.1}$$

Here $\nu_k(x), k \in \{1, ..., N\}$ are neutrino fields in the mass basis with N neutrino mass states. Λ_μ^{kj} is a general vertex function and $A^\mu(x)$ is the electromagnetic field.

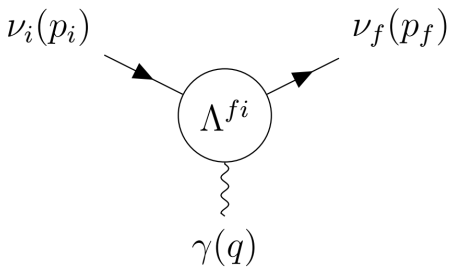

Figure 2.1: Effective coupling of neutrinos with one photon electromagnetic field 2.

The vertex function $\Lambda_\mu^{fi}(q)$ is generally a matrix and in the most general case can be written in terms of linearly independent products of Dirac matrices (γ) and only

depends on the square of the four momentum of the photon ($q = p_f - p_i$):

$$\begin{aligned}\Lambda_{\mu}^{fi}(q) =& \mathbb{F}_1^{fi}\left(q^2\right) q_\mu + \mathbb{F}_2^{fi}\left(q^2\right) q_\mu\gamma_5 + \mathbb{F}_3^{fi}\left(q^2\right)\gamma_\mu + \mathbb{F}_4^{fi}\left(q^2\right)\gamma_\mu\gamma_5 + \\ & \mathbb{F}_5^{fi}\left(q^2\right)\sigma_{\mu\nu}q^\nu + \mathbb{F}_6^{fi}\left(q^2\right)\epsilon_{\mu\nu\rho\gamma}q^\nu\sigma^{\rho\gamma},\end{aligned} \tag{2.2}$$

where $\mathbb{F}_i^{fi}(q^2)$ are six Lorentz invariant form factors [**?**].

Applying conditions of hermiticity $\left(\mathcal{H}_{em}^{(\nu)\dagger} = \mathcal{H}_{em}^{(\nu)}\right)$ and of the gauge invariance of the electromagnetic field, we can rewrite the vertex function as

$$\Lambda_{\mu}^{fi}(q) = \left(\gamma_\mu - q_\mu \not{q}/q^2\right)\left[\mathbb{F}_Q^{fi}\left(q^2\right) + \mathbb{F}_A^{fi}\left(q^2\right)q^2\gamma_5\right] - i\sigma_{\mu\nu}q^\nu\left[\mathbb{F}_M^{fi}\left(q^2\right) + i\mathbb{F}_E^{fi}\left(q^2\right)\gamma_5\right], \tag{2.3}$$

where $\mathbb{F}_Q^{fi}, \mathbb{F}_M^{fi}, \mathbb{F}_E^{fi}$ and $\mathbb{F}_A^{fi}$ are hermitian matrices representing the charge, dipole magnetic, dipole electric and anapole neutrino form factors. In coupling with a real photon ($q^2 = 0$) these become the neutrino charge and magnetic, electric and anapole moments. The neutrino charge radius corresponds to the second term in the expansion of the charge form factor [**?**].

We can simplify the above expression as [**?**]

$$\Lambda_{\mu}^{fi}(q) = \gamma_\mu\left(Q_{\nu_{fi}} + \frac{q^2}{6}\langle r^2\rangle_{\nu_{fi}}\right) - i\sigma_{\mu\nu}q^\nu\mu_{\nu_{fi}}, \tag{2.4}$$

where $Q_{\nu_{fi}}$, $\langle r^2\rangle_{\nu_{fi}}$, and $\mu_{\nu_{fi}}$ are the neutrino charge, effective charge radius (also containing anapole moment), and an effective magnetic moment (also containing electric moment) respectively. This is possible thanks to the proportional effect of the neutrino charge radius and the anapole moment, or the neutrino magnetic and electric moment respectively [**?**]. These quantities (charge, charge radius and magnetic moment) are the three neutrino electromagnetic properties measured in experiments.

2.1.1 Neutrino electric and magnetic dipole moments

The size and effect of the neutrino electromagnetic properties depends on the specific theory beyond the standard model.

Evaluating the one loop diagrams in the minimal extension of the standard model with three right handed Dirac neutrinos gives us the first approximation of the electric

and magnetic moments:

$$\left.\begin{matrix}\mu^D_{kj}\\ i\epsilon^D_{kj}\end{matrix}\right\} \simeq \frac{3eG_F}{16\sqrt{2}\pi^2}\left(m_k \pm m_j\right)\left(\delta_{kj} - \frac{1}{2}\sum_{l=e,\mu,\tau} U^\star_{lk}U_{lj}\frac{m_l^2}{m_W^2}\right), \tag{2.5}$$

where m_k, m_j are the neutrino masses and m_l are the masses of charged leptons which appear in the loop diagrams [**?**]. e is the electron charge, G_F is the Fermi coupling constant, and U is the PMNS neutrino oscillation matrix. Higher order electromagnetic corrections were neglected, but those can also have a significant contribution, depending on the theory.

It can be seen that there dirac neutrinos have no diagonal electric moments $\left(\epsilon^D_{kk} = 0\right)$ and their diagonal magnetic moments are approximately

$$\mu^D_{kk} \simeq \frac{3eG_F m_k}{8\sqrt{2}\pi^2} \simeq 3.2\times 10^{-19}\left(\frac{m_k}{\text{eV}}\right)\mu_B, \tag{2.6}$$

where μ_B is the Bohr magneton [**?**].

The transition magnetic moments are suppressed with respect to the largest of the diagonal magnetic moments by at least a factor of 10^{-4} due to the m_W^2 in the denominator. The transition electric moments are even smaller due to the mass difference in Eq.2.5. Therefore an experimental observation of a magnetic moment larger than in Eq.2.6 would indicate physics beyond the minimally extended standard model [**? ?**].

Majorana neutrinos in a minimal extension can be obtained by either adding a SU $(2)_L$ Higgs triplet, or right handed neutrinos together with a SU $(2)_L$ Higgs singlet [**?**]. If we neglect the Feynman diagrams which depend on the model of the scalar sector, the magnetic and electric dipole moments are

$$\mu^M_{kj} \simeq -\frac{3ieG_F}{16\sqrt{2}\pi^2}\left(m_k + m_j\right)\sum_{l=e,\mu,\tau}\text{Im}\left[U^\star_{lk}U_{lj}\right]\frac{m_l^2}{m_W^2}, \tag{2.7}$$

$$\epsilon^M_{kj} \simeq \frac{3ieG_F}{16\sqrt{2}\pi^2}\left(m_k - m_j\right)\sum_{l=e,\mu,\tau}\text{Re}\left[U^\star_{lk}U_{lj}\right]\frac{m_l^2}{m_W^2}. \tag{2.8}$$

These are difficult to compare to the Dirac case, due to possible presence of Majorana phases in the PMNS matrices, but it is clear that they have the same order of magnitude as Dirac transition dipole moments. However, the neglected model dependent

contributions can enhance the transition dipole moments [?].

It is possible [?] to obtain a "natural" upper limits on the size of neutrino magnetic moment by calculating its contribution to the neutrino mass by standard model radiative corrections. For Dirac neutrinos, the radiative correction induced by neutrino magnetic moment, generated at an energy scale Λ, to the neutrino mass is generically

$$m_\nu^D \sim \frac{\mu_\nu^D}{3 \times 10^{-15} \mu_B} \left[\Lambda \left(\text{TeV}\right)\right]^2 \text{eV}. \tag{2.9}$$

So for $\Lambda \simeq 1$TeV TO DO: *figure out what exactly does this energy scale actually relate to and explain it here?* and $m_\nu \lesssim 0.3$eV the limit becomes $\mu_\nu^D \lesssim 10^{-15} \mu_B$. This applies only if the new physics is well above the electroweak scale ($\Lambda_{EW} \sim 100$GeV). It is possible to get Dirac neutrino magnetic moment higher than this limit, for example in frameworks of minimal super-symmetric standard model, by adding more Higgs doublets, or by considering large extra dimensions [?].

A similar limit for Majorana neutrino magnetic moment would be less stringent due to the antisymmetry of the Majorana neutrino magnetic moment form factors. Considering $m_\nu \lesssim 0.3$eV, the limit can be expressed as

$$\mu_{\tau\mu}, \mu_{\tau e} \lesssim 10^{-9} \left[\Lambda \left(\text{TeV}\right)\right]^{-2} \tag{2.10}$$

$$\mu_{\mu e} \lesssim 3 \times 10^{-7} \left[\Lambda \left(\text{TeV}\right)\right]^{-2} \tag{2.11}$$

which is shown in the flavour basis [?]. This expression relates to the framework used previously as

$$\mu_{ij} = \sum_{\alpha\beta} \mu_{\alpha\beta} U_{\alpha i}^\star U_{\beta j}, \quad \alpha, \beta \in \{e, \mu, \tau\}\,. \tag{2.12}$$

These considerations imply, that if a magnetic moment $\mu \gtrsim 10^{-15} \mu_B$ would be measured, it is more plausible that neutrinos are Majorana fermions and that the scale of lepton violation would be well below the conventional see-saw scale [?] TO DO: *double check this claim*.

Effective neutrino magnetic moment

Since experiments detect neutrino flavour states, not the mass states, what we measure in experiments is an effective "flavour" magnetic moment μ_{eff}. μ_{eff} is influenced by mixing of the neutrino magnetic moments (and electric moments) expressed in the mass basis (as described above) and neutrino oscillations. In the ultra-relativistic limit, the (anti)neutrino effective magnetic moment is

$$\mu_{\nu_l}^2 \left(L, E_\nu\right) = \sum_j \left| \sum_k U_{lk}^\star e^{\mp i \Delta m_{kj}^2 L/2E_\nu} \left(\mu_{jk} - i\epsilon_{jk}\right) \right|^2 , \tag{2.13}$$

where L is the distance the neutrino travelled, E_ν is the neutrino energy and δm^2 is the neutrino mass squared difference [**?**]. The minus sign in the exponent is for neutrinos and the plus sign for antineutrinos, therefore the only difference is in the phase induced by neutrino oscillations.

For experiments with baselines short enough that neutrino oscillations would not have time to develop ($\Delta m^2 L/2E_\nu \ll\sim 1$), such as the NOvA Near Detector, the effective magnetic moment can be expressed as

$$\mu_{\nu_l}^2 = \mu_{\overline{\nu}_l}^2 \simeq \sum_j \left| \sum_k U_{lk}^\star \left(\mu_{jk} - i\epsilon_{jk}\right) \right|^2 = \left[U \left(\mu^2 + \epsilon^2\right) U^\dagger + 2\,\mathrm{Im}\left(U\mu\epsilon U^\dagger\right) \right]_{ll'} , \tag{2.14}$$

which is independent of the neutrino energy and of the source to detector distance.

It is important to mention, that since the effective magnetic moment depends on the flavour of the studied neutrino, it is different (but related) for neutrino experiment studying neutrinos from different sources. Additionally some experiments, namely solar neutrino experiments, need to include matter effects on the neutrino oscillations. Therefore the reports on the value (or upper limit) of the effective neutrino magnetic moment are not directly comparable between different types of neutrino experiments. Theorists publish papers trying to extrapolate the measured effective magnetic moments to each neutrino flavour, but necessarily apply assumptions that might not hold in all BSM theories.

2.1.2 Other neutrino electromagnetic properties

TO DO: *This section is not finished, most of this text is just copied from some theory papers for now*

Neutrino electric charge is heavily constraint by the measurements on the neutrality of matter (since generally neutrinos having an electric charge would also mean that neutrons have charge which would affect all heavier nuclei). It is also constrained by the SN1987A, since neutrino having an effective charge would lengthen its path through the extragalactic magnetic fields and would arrive on earth later. It can also be obtained from nu-on-e scatter from the relationship between neutrino millicharge and magnetic moment. [nuElmagInt2015.pdf - sec. VIIA]

The neutrino charge radius is determined by the second term in the expansion of the neutrino charge form factor and can be interpreted using the Fourier transform of a spherically symmetric charge distribution. It can also be negative since the charge density is not a positively defined quantity. In the SM the charge radius has the form of (possible other definitions exist)

$$\langle r^2_{\nu_l} \rangle_{\mathrm{SM}} = \frac{G_{\mathrm{F}}}{4\sqrt{2}\pi^2} \left[3 - 2 \log \left(\frac{m_l^2}{m_W^2} \right) \right] . \tag{2.15}$$

This corresponds to $\langle r^2_{\nu_\mu} \langle_{\mathrm{SM}} = 2.4 \times 10^{-33}\ \mathrm{cm}^2$ and similar scale for other neutrino flavours. [nuElmagInt2015.pdf - sec. VIIB]

[nuElmagInt2015.pdf - sec. VIIB] The effect of the neutrino charge radius on the neutrino-on-electron scattering cross section is through the following shift of the vector coupling constant (Grau and Grifols, 1986; Degrassi, Sirlin, and VMarciano, 1989; Vogel and Engel, 1989; Hagiwara et al., 1994):

$$g_V^{\nu_l} \to g_V^{\nu_l} + \frac{2}{3} m_W^2 \langle r^2_{\nu_l} \rangle \sin^2 \theta_W \tag{2.16}$$

[nuElmagInt2015.pdf - sec. VIIB] The current experimental limits for muon neutrinos are from TO DO: *check the current exp. limits* Hirsch, Nardi, and Restrepo (2003) who obtained the following 90% C.L. bounds on $\langle r^2_{\nu_\mu} \rangle$ from a reanalysis of CHARM-II (Vilain et al., 1995) and CCFR (McFarland et al.,1998) data:

$$-0.52 \times 10^{-32} < \langle r^2_{\nu_\mu} \rangle < 0.68 \times 10^{-32}\ \mathrm{cm}^2 \tag{2.17}$$

In the Standard Model, the neutrino anapole moment is somehow coupled with the neutrino charge radii and is functionally identical. the phenomenology of neutrino anapole moments is similar to that of neutrino charge radii. Hence, the limits on the neutrino charge radii discussed in Sec. VII.B also apply to the neutrino anapole moments multiplied by 6. in the standard model the neutrino charge radius and the anapole moment are not defined separately and one can interpret arbitrarily the charge form factor as a charge radius or as an anapole moment. Therefore, the standard model values for the neutrino charge radii in Eqs. (7.35)–(7.38) can be interpreted also as values of the corresponding neutrino anapole moments. [nuElmagInt2015.pdf - sec. VIIC]

It is possible to consider the toroidal dipole moment as a characteristic of the neutrino which is more convenient and transparent than the anapole moment for the description of T-invariant interactions with nonconservation of the P and C symmetries. the toroidal and anapole moments coincide in the static limit when the masses of the initial and final neutrino states are equal to each other. The toroidal (anapole) interactions of a Majorana as well as a Dirac neutrino are expected to contribute to the total cross section of neutrino elastic scattering off electrons, quarks, and nuclei. Because of the fact that the toroidal (anapole) interactions contribute to the helicity preserving part of the scattering of neutrinos on electrons, quarks, and nuclei, its contributions to cross sections are similar to those of the neutrino charge radius. In principle, these contributions can be probed and information about toroidal moments can be extracted in low-energy scattering experiments in the future. Different effects of the neutrino toroidal moment are discussed by Ginzburg and Tsytovich (1985), Bukina, Dubovik, and Kuznetsov (1998a, 1998b), and Dubovik and Kuznetsov (1998). In particular, it has been shown that the neutrino toroidal electromagnetic interactions can produce Cherenkov radiation of neutrinos propagating in a medium. [nuElmagInt2015.pdf - sec. VIIC]

2.1.3 Measuring neutrino magnetic moment

The most sensitive method to measure neutrino magnetic moment is the low energy elastic scattering of (anti)neutrinos on electrons [**?**]. The diagram for this interaction is shown on Fig.2.2 showing the two observables, the recoil electron's kinetic energy

$(T_e = E_{e\prime} - m_e)$ and the recoil angle with respect to the incoming neutrino beam (θ).

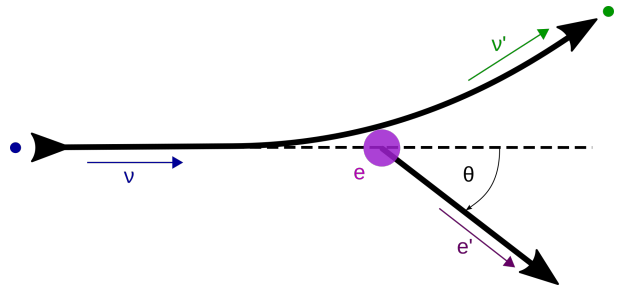

Figure 2.2: Neutrino-on-electron elastic scattering diagram

From simple $2 \to 2$ kinematics we can calculate

$$(P_\nu - P_{e\prime})^2 = (P_{\nu\prime} - P_e)^2 \,, \tag{2.18}$$

$$m_\nu^2 + m_e^2 - 2E_\nu E_{e\prime} + 2E_\nu p_{e\prime} \cos\theta = m_\nu^2 + m_e^2 - 2E_{\nu\prime} m_e. \tag{2.19}$$

Using the energy conservation

$$E_\nu + m_e = E_{\nu\prime} + E_{e\prime} = E_{\nu\prime} + T_e + m_e \Rightarrow E_{\nu\prime} = E_\nu - T_e \tag{2.20}$$

we get

$$E_\nu p_{e\prime} \cos\theta = E_\nu E_{e\prime} - E_{\nu\prime} m_e = E_\nu \left(T_e + m_e\right) - \left(E_\nu - T_e\right) m_e = T_e \left(E_\nu + m_e\right), \tag{2.21}$$

$$\cos\theta = \frac{E_\nu + m_e}{E_\nu} \sqrt{\frac{T_e^2}{E_{e\prime}^2 - m_e^2}} = \frac{E_\nu + m_e}{E_\nu} \sqrt{\frac{T_e^2}{T_e^2 + 2T_e m_e}}. \tag{2.22}$$

And finally we get

$$\cos\theta = \frac{E_\nu + m_e}{E_\nu} \sqrt{\frac{T_e}{T_e + 2m_e}}. \tag{2.23}$$

We can rearrange the Eq. 2.23 to get

$$T_e = \frac{2m_e E_\nu^2 \cos^2\theta}{\left(E_\nu + m_e\right)^2 - E_\nu^2 \cos^2\theta}. \tag{2.24}$$

Electron's kinetic energy is therefore kinematically constrained by the energy conservation as

$$T_e \leq \frac{2E_\nu^2}{2E_\nu + m_e}, \tag{2.25}$$

which corresponds to the $\cos\theta \to 1$ when the recoil electron goes exactly forward in the incident neutrino direction.

Considering $E_\nu \sim$ GeV, we can approximate $\frac{m_e^2}{E_\nu^2} \to 0$ and from Fig.2.3 we can see that we can approximate all recoil angles to be very small, therefore $\theta^2 \cong (1 - \cos^2\theta)$. Using Eq.2.23 we get

$$T_e\theta^2 \cong T_e\left(1 - \left(\frac{E_\nu + m_e}{E_\nu}\right)^2 \frac{T_e}{T_e + 2m_e}\right) = T_e\left(1 - \left(1 + \frac{2m_e}{E_\nu}\right)\frac{T_e}{T_e + 2m_e}\right), \tag{2.26}$$

therefore

$$T_e\theta^2 \cong \frac{2m_eT_e}{T_e + 2m_e}\left(1 - \frac{T_e}{E_\nu}\right) = 2m_e\left(\frac{1}{1 + \frac{2m_e}{T_e}}\right)\left(1 - \frac{T_e}{E_\nu}\right), \tag{2.27}$$

and finally

$$T_e\theta^2 \cong 2m_e\left(1 - \frac{T_e}{E_\nu}\right) < 2m_e. \tag{2.28}$$

This is a strong limit that clearly distinguishes the neutrino-on-electron elastic scattering events from other similar interaction involving single electron (mainly the ν_e Charged Current interaction).

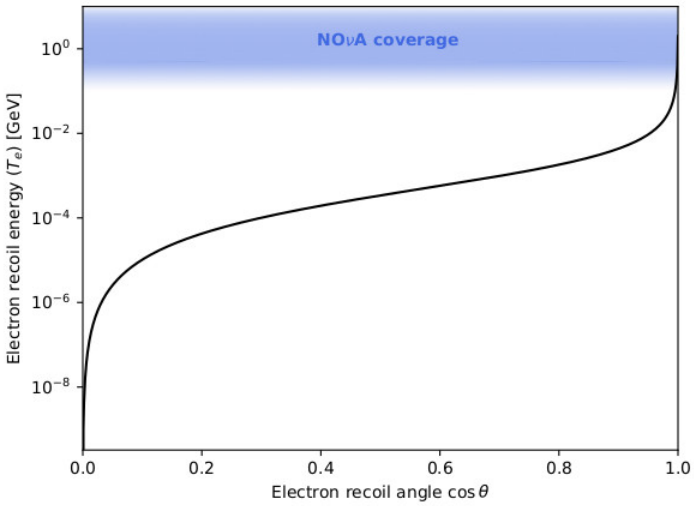

Figure 2.3: Relation between the recoil electron's kinetic energy and angle for neutrino-on-electron elastic scattering. The coverage of the NOvA detectors for measuring the electron recoil energy is shown in blue. Only very forwards electron's are recorded in NOvA.

Neutrino magnetic moment cross section

In the ultrarelativistic limit, the neutrino magnetic moment changes the neutrino helicity, turning active neutrinos into sterile TO DO: *this is a very strong statement and it probably need a bit more backing up*. Since the SM weak interaction conserves helicity we can simply add the two contribution to the neutrino-on-electron cross section incoherently [**?**]:

$$\frac{d\sigma_{\nu_l e^-}}{dT_e} = \left(\frac{d\sigma_{\nu_l e^-}}{dT_e}\right)_{\text{SM}} + \left(\frac{d\sigma_{\nu_l e^-}}{dT_e}\right)_{\text{MAG}}. \tag{2.29}$$

The standard model contribution can be expressed as [**?**]:

$$\left(\frac{d\sigma_{\nu_l e^-}}{dT_e}\right)_{\text{SM}} = \frac{G_F^2 m_e}{2\pi}\left\{(g_V^{\nu_l}+g_A^{\nu_l})^2 + (g_V^{\nu_l}-g_A^{\nu_l})^2\left(1-\frac{T_e}{E_\nu}\right)^2 + \left((g_A^{\nu_l})^2-(g_V^{\nu_l})^2\right)\frac{m_e T_e}{E_\nu^2}\right\}, \tag{2.30}$$

where the coupling constants g_V and g_A are different for different neutrino flavours and for antineutrinos. Their values are:

$$g_V^{\nu_e} = 2\sin^2\theta_W + 1/2, \qquad g_A^{\nu_e} = 1/2, \tag{2.31}$$

$$g_V^{\nu_{\mu,\tau}} = 2\sin^2\theta_W - 1/2, \qquad g_A^{\nu_{\mu,\tau}} = -1/2. \tag{2.32}$$

For antineutrinos $g_A \to -g_A$.

Using Eq. 2.24 to get the differential cross section on $\cos\theta$:

$$dT_e = \frac{4m_e E_\nu^2 (m_e+E_\nu)^2}{\left[(m_e+E_\nu)^2 - E_\nu^2\cos^2\theta\right]^2}\cos\theta d\cos\theta \tag{2.33}$$

We can also express this as

$$\left(\frac{d\sigma_{\nu_l e^-}}{d\cos\theta}\right)_{\text{SM}} = \frac{2G_F^2 E_\nu^2 m_e^2\cos\theta\,(E_\nu+m_e)^2}{\pi\left((E_\nu+m_e)^2 - E_\nu^2\cos^2\theta\right)^2} \left\{(g_V^{\nu_l}+g_A^{\nu_l})^2 + (g_V^{\nu_l}-g_A^{\nu_l})^2\left(1-\frac{2m_e E_\nu\cos^2\theta}{(E_\nu+m_e)^2-E_\nu^2\cos^2\theta}\right)^2 + \left((g_A^{\nu_l})^2-(g_V^{\nu_l})^2\right)\frac{2m_e^2\cos^2\theta}{\left((E_\nu+m_e)^2-E_\nu^2\cos^2\theta\right)}\right\}, \tag{2.34}$$

ht

Table 2.1: Neutrino-on-electron elastic scattering total cross sections

Process	Total cross section
$\nu_e + e^-$	$\simeq 93 \times 10^{-43} E_\nu \mathrm{cm}^2 \mathrm{GeV}^{-1}$
$\overline{\nu}_e + e^-$	$\simeq 39 \times 10^{-43} E_\nu \, \mathrm{cm}^2 \mathrm{GeV}^{-1}$
$\nu_{\mu,\tau} + e^-$	$\simeq 15 \times 10^{-43} E_\nu \, \mathrm{cm}^2 \mathrm{GeV}^{-1}$
$\overline{\nu}_{\mu,\tau} + e^-$	$\simeq 13 \times 10^{-43} E_\nu \, \mathrm{cm}^2 \mathrm{GeV}^{-1}$

[Fundamentals of neutrino Physics and Astrophysics, p.139] The total neutrino-electron elastic scattering cross section for large energies is

The neutrino magnetic moment contribution is TO DO: *include derivation from [?]* [?]:

$$\left(\frac{d\sigma_{\nu_l e^-}}{dT_e}\right)_{\mathrm{MAG}} = \frac{\pi\alpha^2}{m_e^2}\left(\frac{1}{T_e} - \frac{1}{E_\nu}\right)\left(\frac{\mu_{\nu_l}}{\mu_B}\right)^2 , \tag{2.35}$$

where α is the fine structure constant.

Comparison of the Standard Model and the neutrino magnetic moment cross sections is shown on Fig.2.4. Whereas the SM cross section is flat with $T_e \to 0$, the νMM cross section keeps increasing to infinity. However, this reach is limited by the experimental capabilities of detecting such low energetic neutrinos. Possible NOvA coverage is shown in a shaded blue and it is uncertain we could actually reach as low as 100 MeV.

TO DO: *Reference the colours on the figures to the origins of the values (LSND and Biao)*

As can be seen on Fig.2.4 and Fig.2.5, the magnetic moment contribution exceeds the standard model contribution for low enough T_e. This can be approximated as [?]:

$$T_e \lesssim \frac{\pi^2\alpha^2}{G_F^2 m_e^3}\left(\frac{\mu_\nu}{\mu_B}\right)^2 \simeq 2.9 \times 10^{19}\left(\frac{\mu_\nu}{\mu_B}\right)^2 [\mathrm{MeV}] , \tag{2.36}$$

which does not depend on the neutrino energy and makes experiments sensitive to lower energetic electrons more sensitive to the neutrino magnetic moment. This is especially true for the recent dark matter experiments which put stringent limits on the solar neutrino effective magnetic moment, as described in the following section.

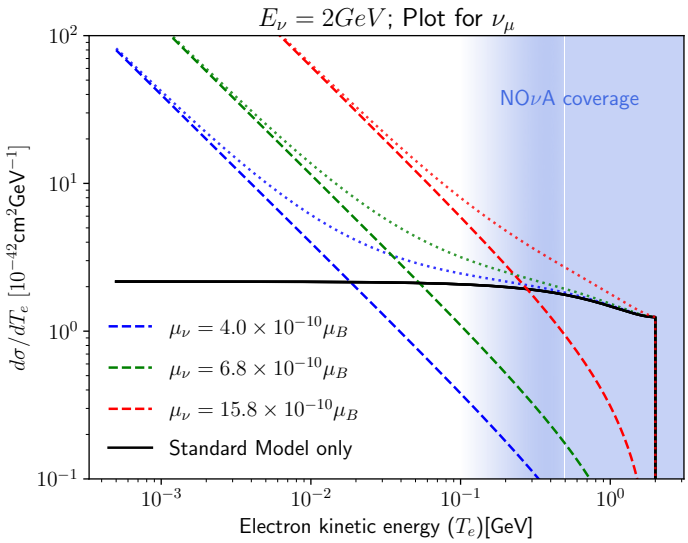

Figure 2.4: Comparison of the neutrino magnetic moment (coloured) and Standard Model (black) cross sections for the neutrino-on-electron elastic scattering. Different colours depict different values of the neutrino magnetic moment. Dashed lines are the individual cross sections and dotted lines are the added total cross section with the standard model contribution. NOvA coverage of electron recoil energies is shown in shaded blue.

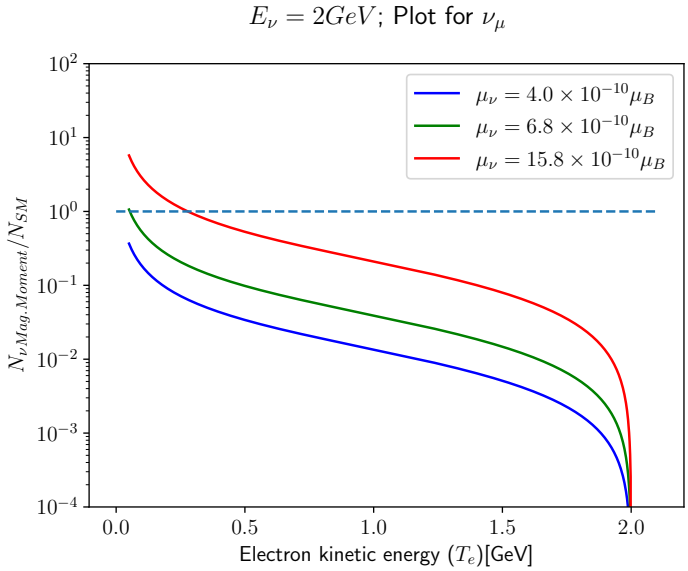

Figure 2.5: Ratio of the netrino magnetic moment cross section to the standard model cross section for the neutrino-on-electron elastic scattering. Different colours depict different effective muon neutrino magnetic moment values.

Acronyms

CC Charged current. 2, 3, 6, 8

CP Charge conjugation - Parity (symmetry). 10

DIS Deep Inelastic Scattering. 5

FSI Final State Interaction. 5

MEC Meson Exchange Current. 5

NC Neutral Current. 2–4

PMNS Pontecorvo Maki Nakagawa Sakata. 8, 10

QE Quasi Elastic (interaction). 5

QED Quantum Electro Dynamics. 5

SM Standard Model. 2, 3

Bibliography

[1] Wolfgang Pauli. Pauli letter collection: letter to Lise Meitner. Typed copy. URL http://cds.cern.ch/record/83282.

[2] L. M. Brown. The idea of the neutrino. *Physics Today*, 31(9):23–28, September 1978. doi:10.1063/1.2995181. (Including translation of W. Pauli, Aufsdtze und Vortrdge u'ber Physik und Erkenntnistheorie, Braunschweig (1961)).

[3] H. A. Bethe. Ionization power of a neutrino with magnetic moment. *Mathematical Proceedings of the Cambridge Philosophical Society*, 31(1):108–115, 1935. doi:10.1017/S0305004100012998.

[4] Enrico Fermi. Tentativo di una teoria dei raggi β. 11(1):1–19. ISSN 1827-6121. doi:10.1007/BF02959820.

[5] Fred L. Wilson. Fermi's theory of beta decay. *American Journal of Physics*, 36 (12):1150–1160, 1968. doi:10.1119/1.1974382. (A complete English translation of E.Fermi, Zeitschrift fur Physik 88, 161 (1934)).

[6] Sheldon L. Glashow. Partial-symmetries of weak interactions. 22(4):579–588. ISSN 0029-5582. doi:https://doi.org/10.1016/0029-5582(61)90469-2. URL https://www.sciencedirect.com/science/article/pii/0029558261904692.

[7] Steven Weinberg. A model of leptons. *Phys. Rev. Lett.*, 19:1264–1266, Nov 1967. doi:10.1103/PhysRevLett.19.1264. URL https://link.aps.org/doi/10.1103/PhysRevLett.19.1264.

[8] Abdus Salam. *Weak and electromagnetic interactions*, pages 244–254. doi:10.1142/9789812795915_0034. URL https://www.worldscientific.com/doi/abs/10.1142/9789812795915_0034.

[9] L. Landau. On the conservation laws for weak interactions. 3(1):127–131. ISSN 0029-5582. doi:https://doi.org/10.1016/0029-5582(57)90061-5. URL https://www.sciencedirect.com/science/article/pii/0029558257900615.

[10] T. D. Lee and C. N. Yang. Parity nonconservation and a two-component theory of the neutrino. *Phys. Rev.*, 105:1671–1675, Mar 1957.

doi:10.1103/PhysRev.105.1671. URL https://link.aps.org/doi/10.1103/PhysRev.105.1671.

[11] Abdus Salam. On parity conservation and neutrino mass. *Nuovo Cim.*, 5:299–301, 1957. doi:10.1007/BF02812841.

[12] Peter W. Higgs. Broken symmetries and the masses of gauge bosons. *Phys. Rev. Lett.*, 13:508–509, Oct 1964. doi:10.1103/PhysRevLett.13.508. URL https://link.aps.org/doi/10.1103/PhysRevLett.13.508.

[13] F. Englert and R. Brout. Broken symmetry and the mass of gauge vector mesons. *Phys. Rev. Lett.*, 13:321–323, Aug 1964. doi:10.1103/PhysRevLett.13.321. URL https://link.aps.org/doi/10.1103/PhysRevLett.13.321.

[14] G. S. Guralnik, C. R. Hagen, and T. W. B. Kibble. Global conservation laws and massless particles. *Phys. Rev. Lett.*, 13:585–587, Nov 1964. doi:10.1103/PhysRevLett.13.585. URL https://link.aps.org/doi/10.1103/PhysRevLett.13.585.

[15] Steven Weinberg. A model of leptons. *Phys. Rev. Lett.*, 19:1264–1266, Nov 1967. doi:10.1103/PhysRevLett.19.1264. URL https://link.aps.org/doi/10.1103/PhysRevLett.19.1264.

[16] Carlo Giunti and Chung W. Kim. *Fundamentals of Neutrino Physics and Astrophysics*. 2007. ISBN 978-0-19-850871-7.

[17] F. Reines and C. L. Cowan. Detection of the free neutrino. *Phys. Rev.*, 92:830–831, Nov 1953. doi:10.1103/PhysRev.92.830. URL https://link.aps.org/doi/10.1103/PhysRev.92.830.

[18] Cowan Jr. C.L., Reines F., Harrison F.B., Kruse H.W., and McGuire A.D. Detection of the free neutrino: A confirmation. *Science*, 124(3212):103–104, July 1956. doi:10.1126/science.124.3212.103.

[19] F. Reines and C.L. Cowan. Neutrino physics. *Physics Today*, 10(8):12–18, 1957. doi:10.1063/1.3060455.

[20] B. Adeva et al. Measurement of Z^0 decays to hadrons and a precise determination of the number of neutrino species. *Phys. Lett. B*, 237:136–146, 1990. doi:10.1016/0370-2693(90)90476-M.

[21] S. Schael et al. Precision electroweak measurements on the Z resonance. *Phys. Rept.*, 427:257–454, 2006. doi:10.1016/j.physrep.2005.12.006.

[22] M. C. Goodman. Resource letter anp-1: Advances in neutrino physics. *American Journal of Physics*, 84:309–319, 2016. doi:10.1119/1.4962228.

[23] M. Schwartz. Feasibility of using high-energy neutrinos to study the weak interactions. *Phys. Rev. Lett.*, 4:306–307, Mar 1960. doi:10.1103/PhysRevLett.4.306. URL https://link.aps.org/doi/10.1103/PhysRevLett.4.306.

[24] K. Kodama et al. Observation of tau neutrino interactions. *Phys. Lett. B*, 504: 218–224, 2001. doi:10.1016/S0370-2693(01)00307-0.

[25] K. Kodama et al. Final tau-neutrino results from the DONuT experiment. *Phys. Rev. D*, 78:052002, 2008. doi:10.1103/PhysRevD.78.052002.

[26] William J Marciano and Zohreh Parsa. Neutrino–electron scattering theory*. 29(11):2629. doi:10.1088/0954-3899/29/11/013. URL https://dx.doi.org/10.1088/0954-3899/29/11/013.

[27] D. Akimov, J. B. Albert, P. An, C. Awe, P. S. Barbeau, B. Becker, V. Belov, A. Brown, A. Bolozdynya, B. Cabrera-Palmer, M. Cervantes, J. I. Collar, R. J. Cooper, R. L. Cooper, C. Cuesta, D. J. Dean, J. A. Detwiler, A. Eberhardt, Y. Efremenko, S. R. Elliott, E. M. Erkela, L. Fabris, M. Febbraro, N. E. Fields, W. Fox, Z. Fu, A. Galindo-Uribarri, M. P. Green, M. Hai, M. R. Heath, S. Hedges, D. Hornback, T. W. Hossbach, E. B. Iverson, L. J. Kaufman, S. Ki, S. R. Klein, A. Khromov, A. Konovalov, M. Kremer, A. Kumpan, C. Leadbetter, L. Li, W. Lu, K. Mann, D. M. Markoff, K. Miller, H. Moreno, P. E. Mueller, J. Newby, J. L. Orrell, C. T. Overman, D. S. Parno, S. Penttila, G. Perumpilly, H. Ray, J. Raybern, D. Reyna, G. C. Rich, D. Rimal, D. Rudik, K. Scholberg, B. J. Scholz, G. Sinev, W. M. Snow, V. Sosnovtsev, A. Shakirov, S. Suchyta, B. Suh, R. Tayloe, R. T. Thornton, I. Tolstukhin, J. Vanderwerp, R. L. Varner, C. J. Virtue, Z. Wan, J. Yoo, C.-

H. Yu, A. Zawada, J. Zettlemoyer, A. M. Zderic, and COHERENT Collaboration. Observation of coherent elastic neutrino-nucleus scattering. 357(6356): 1123–1126. doi:10.1126/science.aao0990. URL https://www.science.org/doi/abs/10.1126/science.aao0990.

[28] *Fundamental Physics at the Intensity Frontier*, 5 2012. doi:10.2172/1042577.

[29] J. A. Formaggio and G. P. Zeller. From ev to eev: Neutrino cross sections across energy scales. *Rev. Mod. Phys.*, 84:1307–1341, Sep 2012. doi:10.1103/RevModPhys.84.1307. URL https://link.aps.org/doi/10.1103/RevModPhys.84.1307.

[30] D. Casper. The Nuance neutrino physics simulation, and the future. *Nucl. Phys. B Proc. Suppl.*, 112:161–170, 2002. doi:10.1016/S0920-5632(02)01756-5.

[31] Jr. Davis, Raymond, Don S. Harmer, and Kenneth C. Hoffman. Search for neutrinos from the sun. *Phys. Rev. Lett.*, 20:1205–1209, 1968. doi:10.1103/PhysRevLett.20.1205.

[32] G. Danby, J-M. Gaillard, K. Goulianos, L. M. Lederman, N. Mistry, M. Schwartz, and J. Steinberger. Observation of high-energy neutrino reactions and the existence of two kinds of neutrinos. *Phys. Rev. Lett.*, 9:36–44, Jul 1962. doi:10.1103/PhysRevLett.9.36. URL https://link.aps.org/doi/10.1103/PhysRevLett.9.36.

[33] C.V. Achar, M.G.K. Menon, V.S. Narasimham, P.V.Ramana Murthy, B.V. Sreekantan, K. Hinotani, S. Miyake, D.R. Creed, J.L. Osborne, J.B.M. Pattison, and A.W. Wolfendale. Detection of muons produced by cosmic ray neutrinos deep underground. 18(2):196–199. ISSN 0031-9163. doi:https://doi.org/10.1016/0031-9163(65)90712-2. URL https://www.sciencedirect.com/science/article/pii/0031916365907122.

[34] C. V. Achar et al. Observation of a non-elastic cosmic ray neutrino interaction. *Phys. Lett.*, 19:78–80, 1965. doi:10.1016/0031-9163(65)90969-8.

[35] F. Reines, M. F. Crouch, T. L. Jenkins, W. R. Kropp, H. S. Gurr, G. R. Smith, J. P. F. Sellschop, and B. Meyer. Evidence for high-energy cosmic-ray neutrino inter-

actions. *Phys. Rev. Lett.*, 15:429–433, Aug 1965. doi:10.1103/PhysRevLett.15.429. URL https://link.aps.org/doi/10.1103/PhysRevLett.15.429.

[36] Y. Fukuda et al. Solar neutrino data covering solar cycle 22. *Phys. Rev. Lett.*, 77:1683–1686, Aug 1996. doi:10.1103/PhysRevLett.77.1683. URL https://link.aps.org/doi/10.1103/PhysRevLett.77.1683.

[37] Q.R. Ahmad et al. Direct evidence for neutrino flavor transformation from neutral current interactions in the Sudbury Neutrino Observatory. *Phys. Rev. Lett.*, 89:011301, 2002. doi:10.1103/PhysRevLett.89.011301.

[38] M. Aglietta et al. Experimental study of atmospheric neutrino flux in the NUSEX experiment. *Europhysics Letters (EPL)*, 8(7):611–614, apr 1989. doi:10.1209/0295-5075/8/7/005. URL https://doi.org/10.1209%2F0295-5075%2F8%2F7%2F005.

[39] K. Daum et al. Determination of the atmospheric neutrino spectra with the fréjus detector. *Zeitschrift für Physik C Particles and Fields*, 66(3):417–428, 1995. ISSN 1431-5858. URL https://doi.org/10.1007/BF01556368.

[40] R. Becker-Szendy et al. Electron- and muon-neutrino content of the atmospheric flux. *Phys. Rev. D*, 46:3720–3724, Nov 1992. doi:10.1103/PhysRevD.46.3720. URL https://link.aps.org/doi/10.1103/PhysRevD.46.3720.

[41] Y. Fukuda et al. Atmospheric ν_μ/ν_e ratio in the multi-GeV energy range. *Phys. Lett. B*, 335(GIFU-PH-94-01. ICRR-321. INS-Rep-1035. KEK-Preprint-94-50. KOBE-AP-94-01. NGTHEP-94-1. OULNS-94-01. TIT-HPE-94-04. TKU-PAP-94-2. UPR-0226-E):237–245. 25 p, Jun 1994. URL https://cds.cern.ch/record/266736.

[42] Y. Fukuda et al. Evidence for oscillation of atmospheric neutrinos. *Phys. Rev. Lett.*, 81:1562–1567, 1998. doi:10.1103/PhysRevLett.81.1562.

[43] B Pontecorvo. Mesonium and antimesonium. *Sov. Phys. JETP*, 33:549–551, 8 1957.

[44] B. Pontecorvo. Inverse beta processes and nonconservation of lepton charge. *Sov. Phys. JETP*, 7:172–173, 1958.

[45] Ziro Maki, Masami Nakagawa, and Shoichi Sakata. Remarks on the unified model of elementary particles. *Prog. Theor. Phys.*, 28:870–880, 1962. doi:10.1143/PTP.28.870.

[46] V. Gribov and B. Pontecorvo. Neutrino astronomy and lepton charge. 28(7):493–496. ISSN 0370-2693. doi:https://doi.org/10.1016/0370-2693(69)90525-5. URL https://www.sciencedirect.com/science/article/pii/0370269369905255.

[47] M.C. Gonzalez-Garcia and Yosef Nir. Neutrino Masses and Mixing: Evidence and Implications. *Rev. Mod. Phys.*, 75:345–402, 2003. doi:10.1103/RevModPhys.75.345.

[48] M. Tanabashi et al. Review of Particle Physics. *Phys. Rev. D*, 98(3):030001, 2018. doi:10.1103/PhysRevD.98.030001. 2019 update.

[49] L. Wolfenstein. Neutrino oscillations in matter. *Phys. Rev. D*, 17:2369–2374, May 1978. doi:10.1103/PhysRevD.17.2369. URL https://link.aps.org/doi/10.1103/PhysRevD.17.2369.

[50] S.P. Mikheyev and A.Yu. Smirnov. Resonance Amplification of Oscillations in Matter and Spectroscopy of Solar Neutrinos. *Sov. J. Nucl. Phys.*, 42:913–917, 1985.

[51] *1st CERN - CLAF School of High-energy Physics*, Geneva, 2003. CERN, CERN. doi:10.5170/CERN-2003-003. URL http://cds.cern.ch/record/485010.

Appendix A

Test Beam Calibration Validation Plots

A.1 Distributions for Stopping Muons

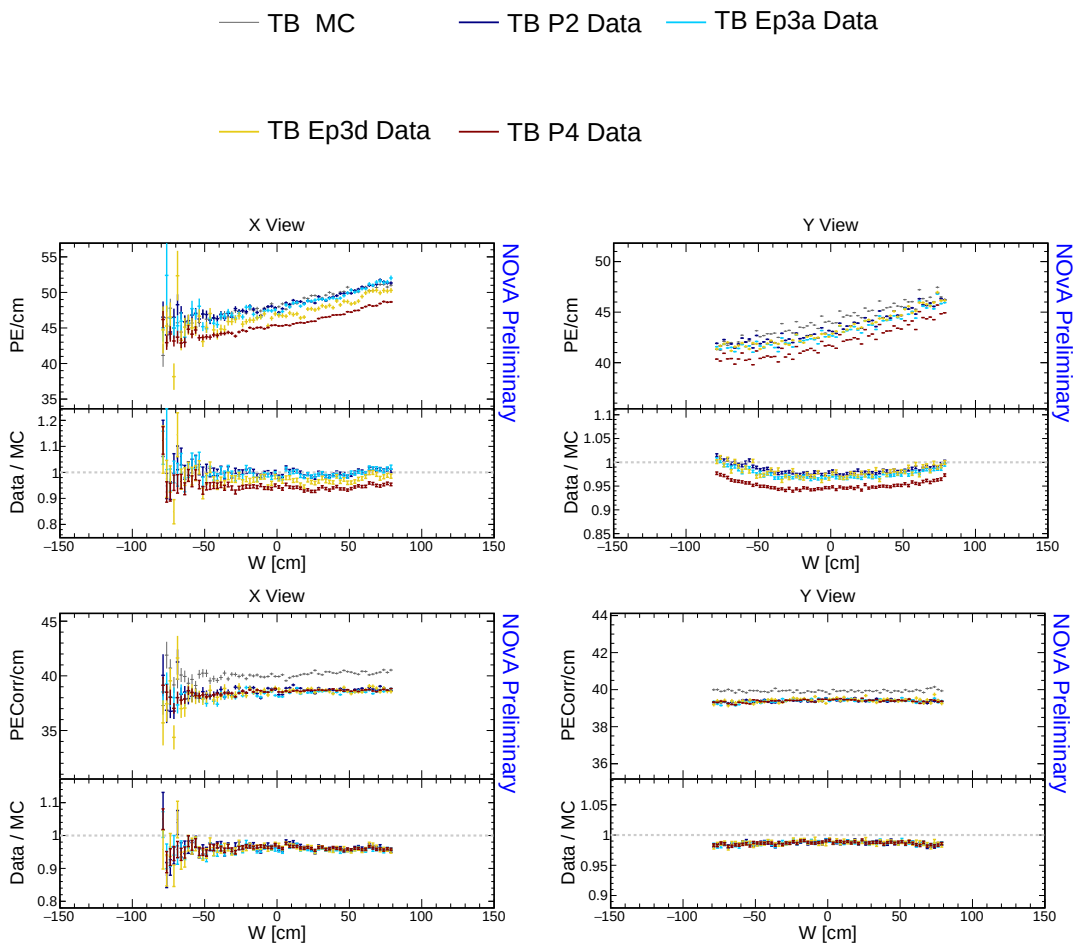

Figure A.1: Distributions of stopping muons within a 1-2 m track window from the end of their tracks across the position within a cell.

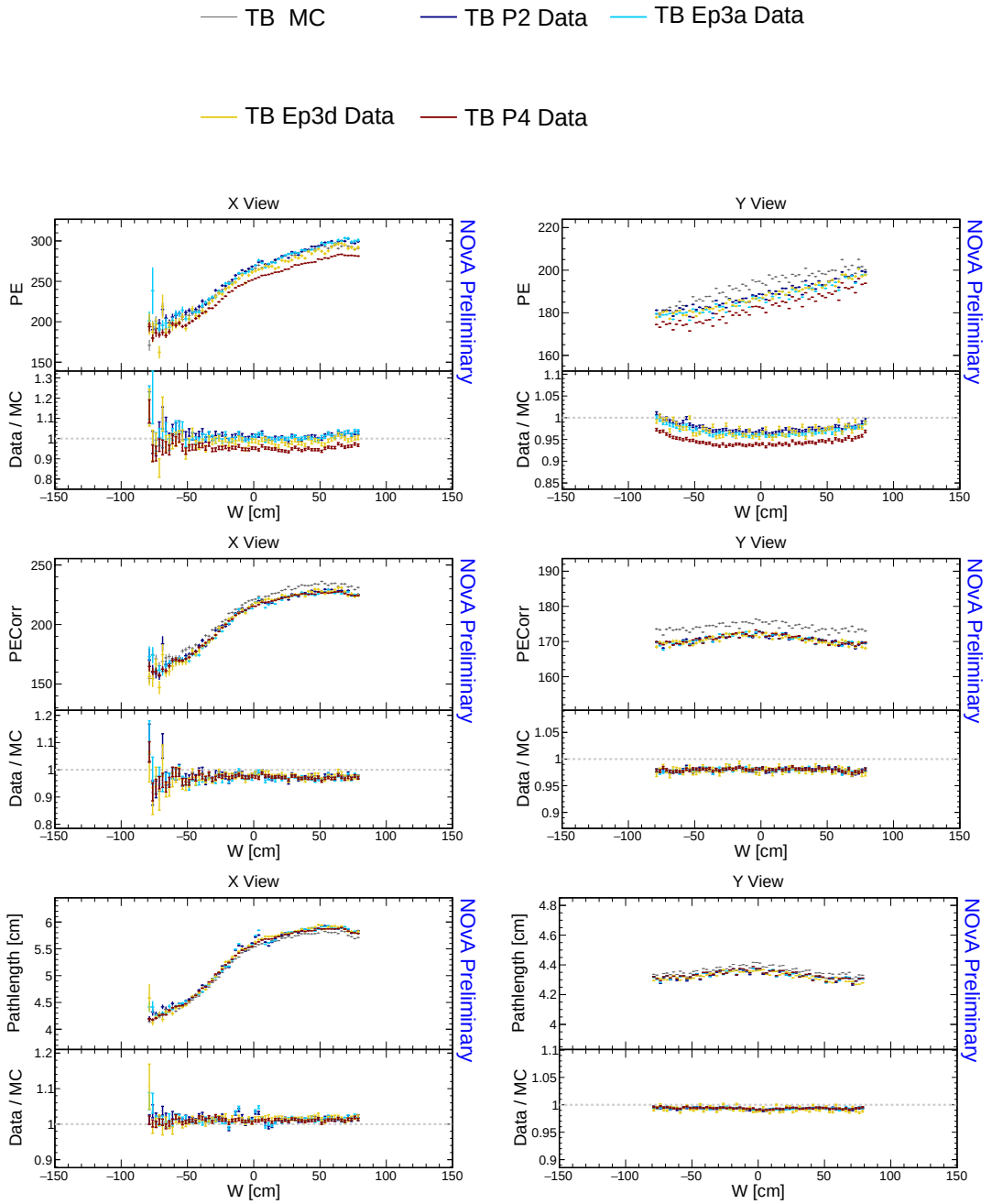

Figure A.2: Distributions of stopping muons within a 1-2 m track window from the end of their tracks across the position within a cell.

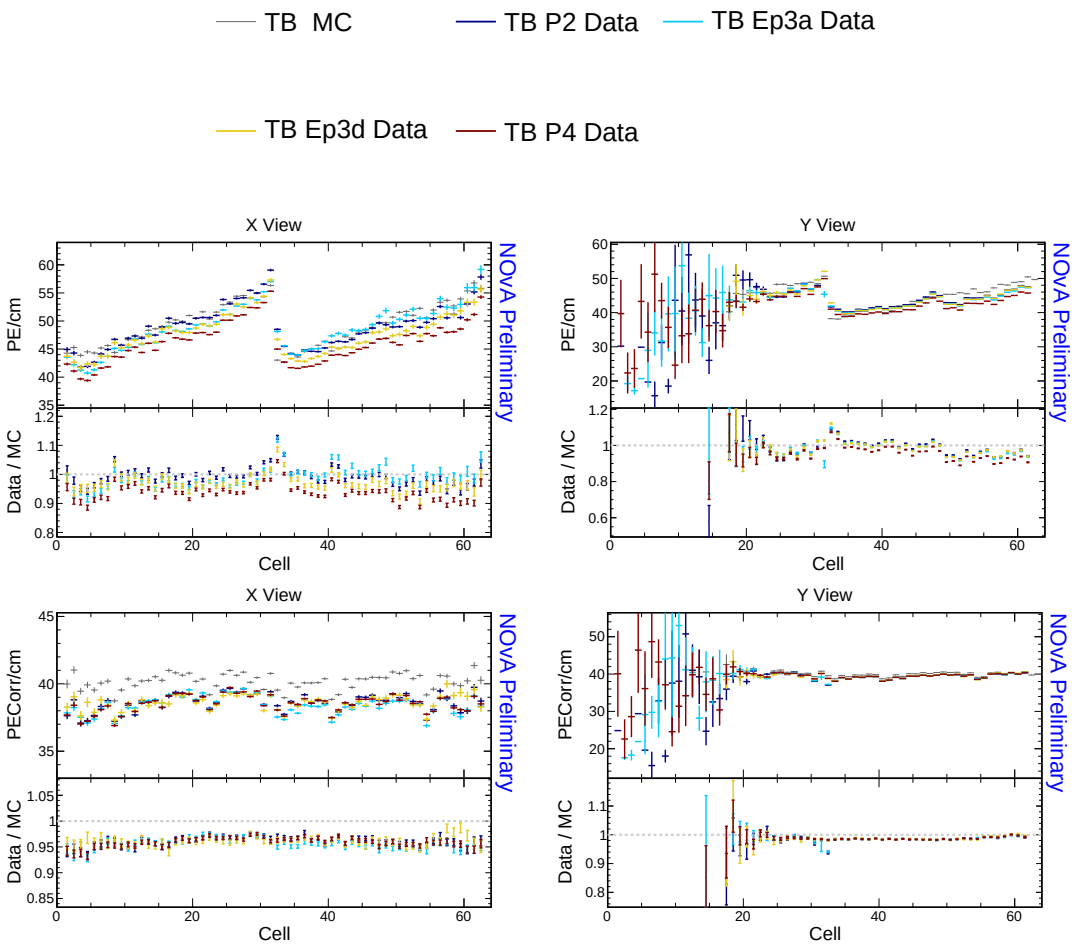

Figure A.3: Distributions of stopping muons within a 1-2 m track window from the end of their tracks across the cells of the detector.

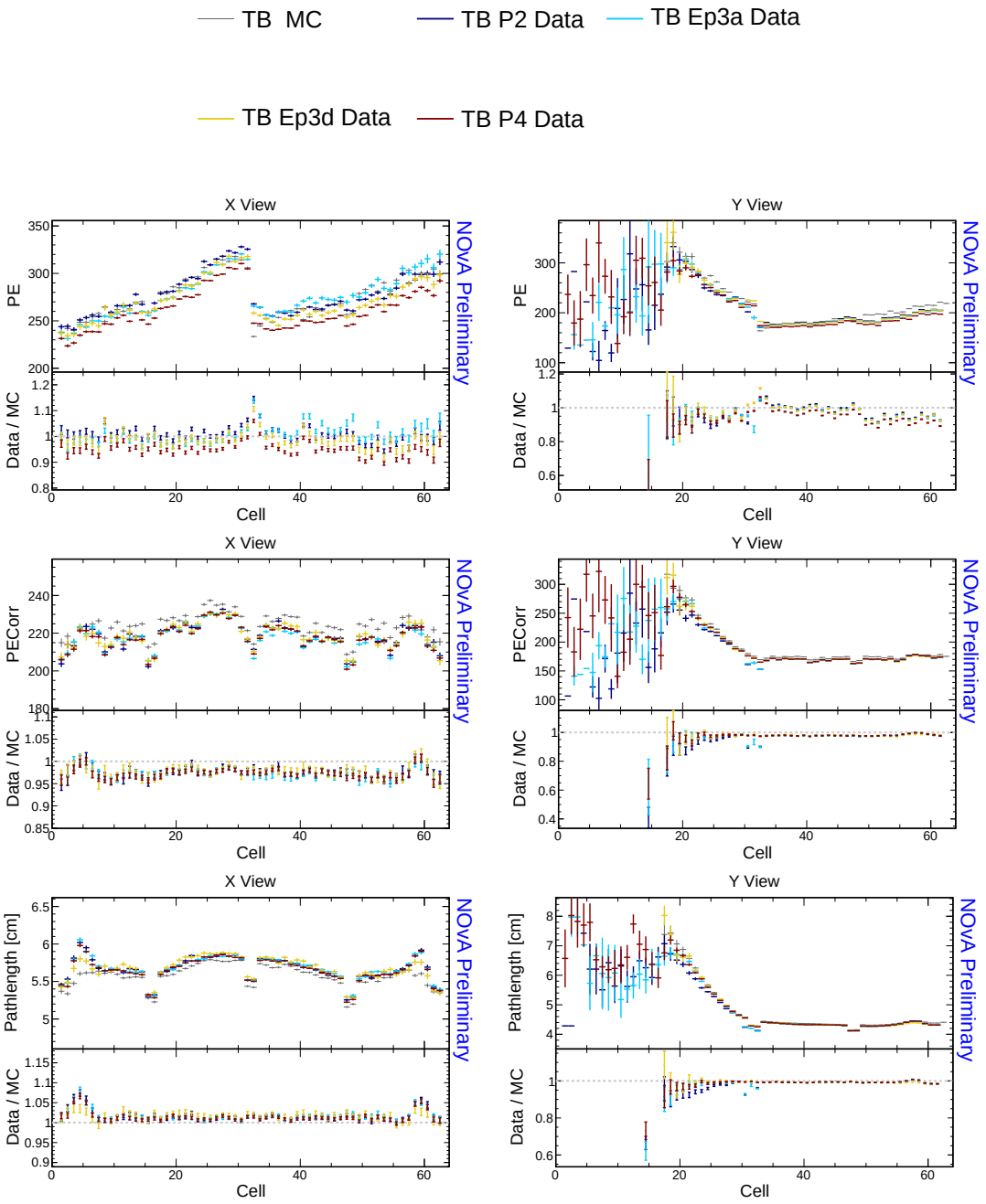

Figure A.4: Distributions of stopping muons within a 1-2 m track window from the end of their tracks across the cells of the detector.

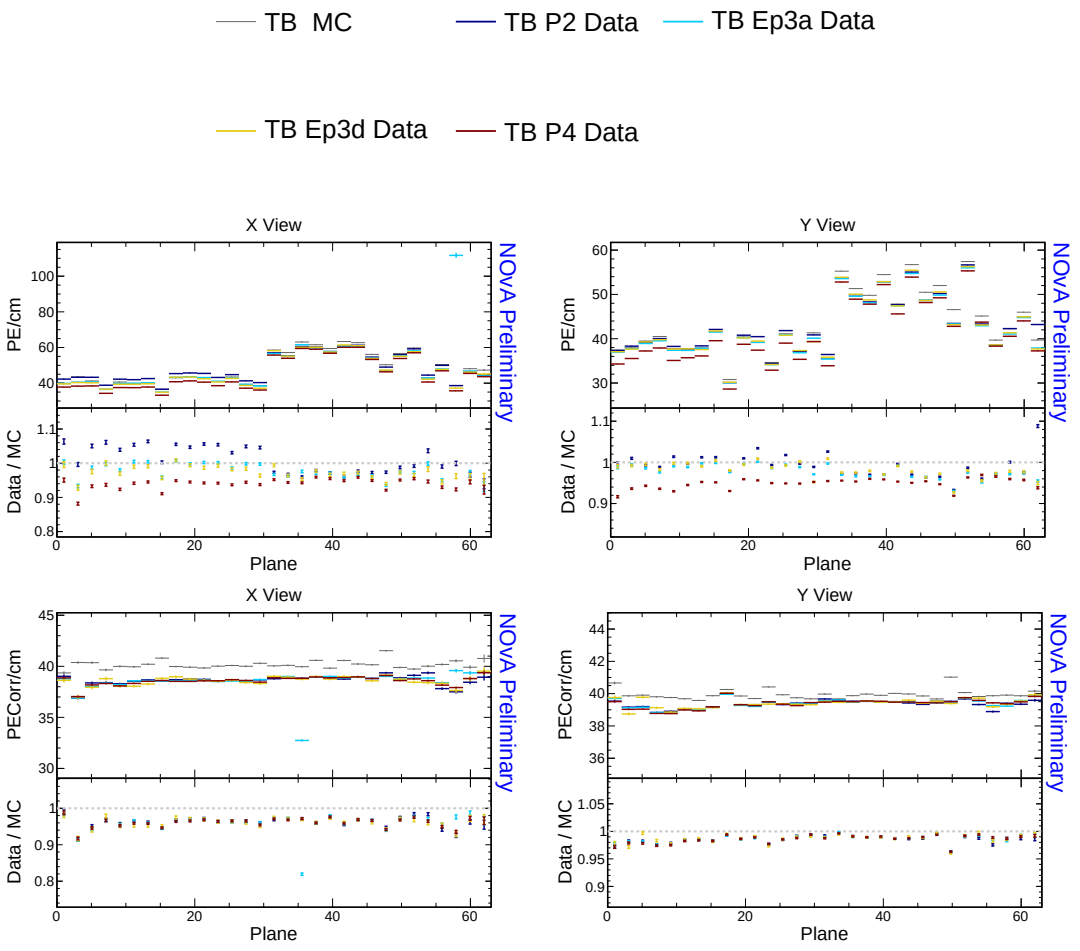

Figure A.5: Distributions of stopping muons within a 1-2 m track window from the end of their tracks across the planes of the detector.

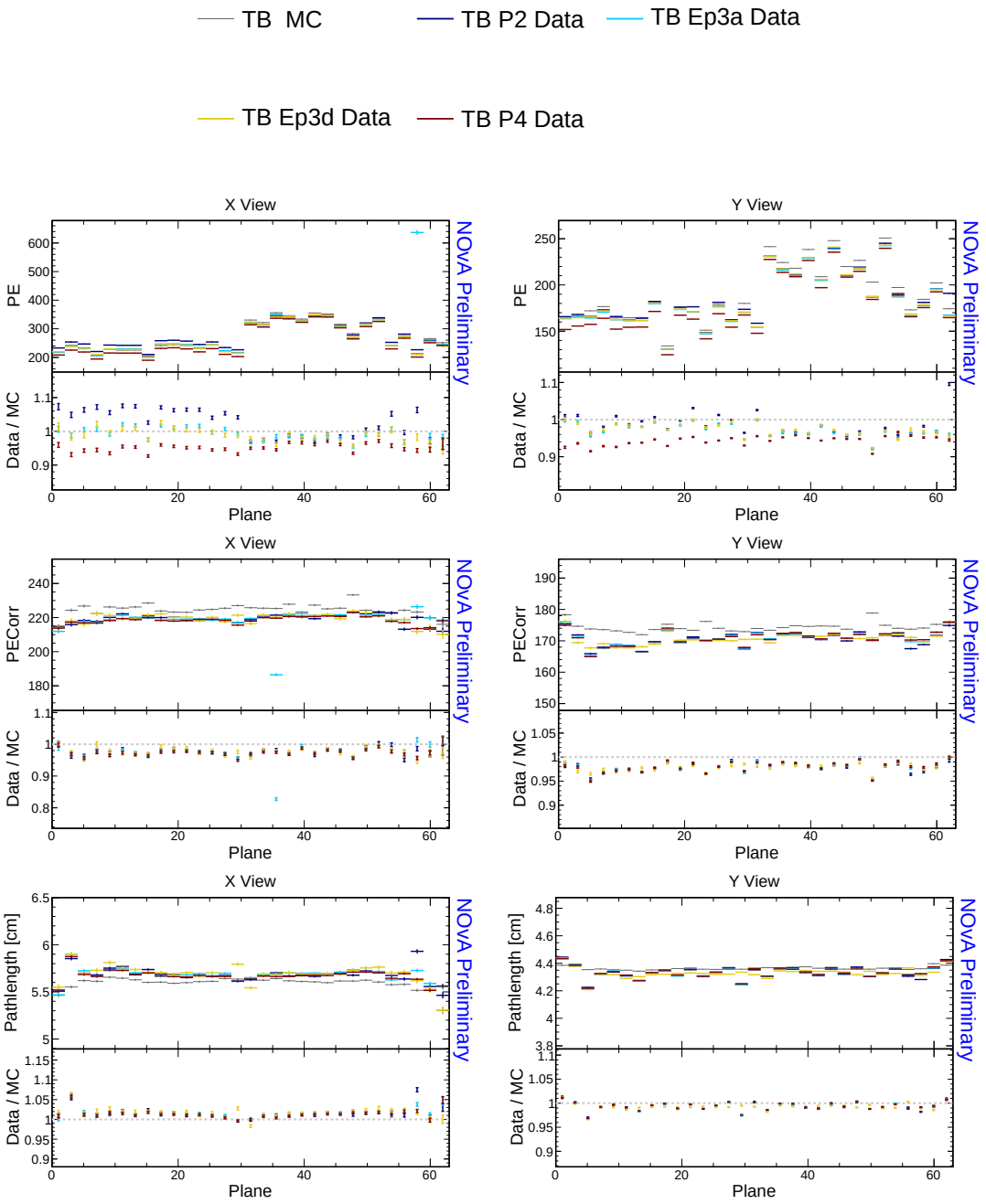

Figure A.6: Distributions of stopping muons within a 1-2 m track window from the end of their tracks across the planes of the detector.

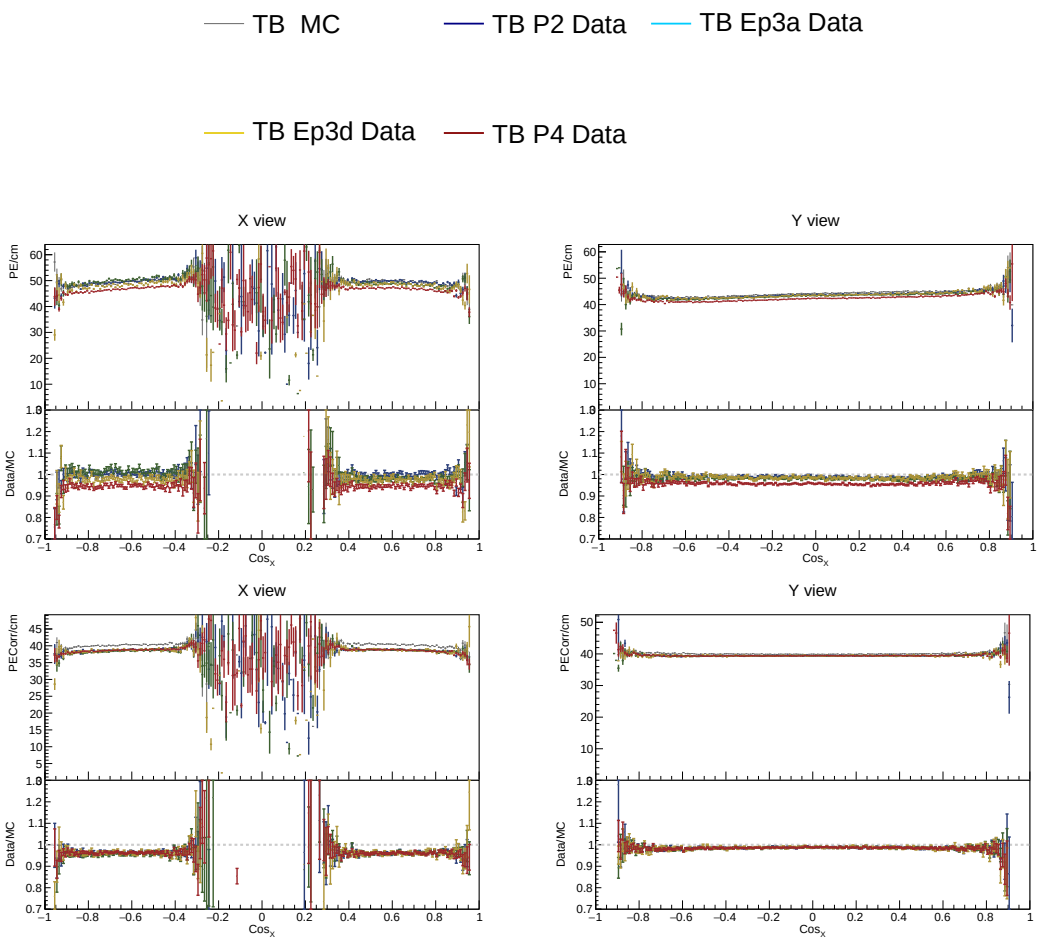

Figure A.7: Distributions of stopping muons within a 1-2 m track window from the end of their tracks across the cosine of the track angle from the X (horizontal) axis.

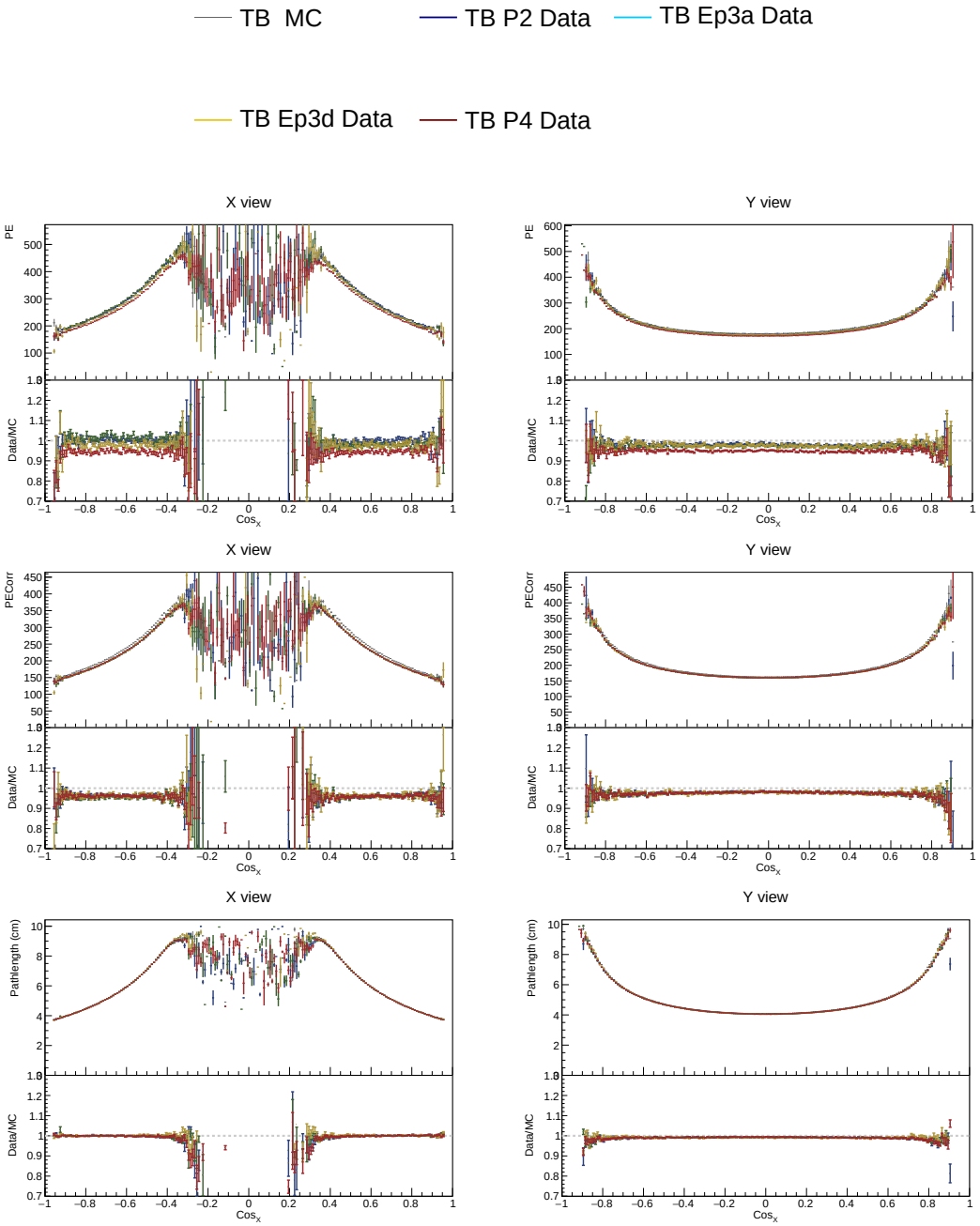

Figure A.8: Distributions of stopping muons within a 1-2 m track window from the end of their tracks across the cosine of the track angle from the X (horizontal) axis.

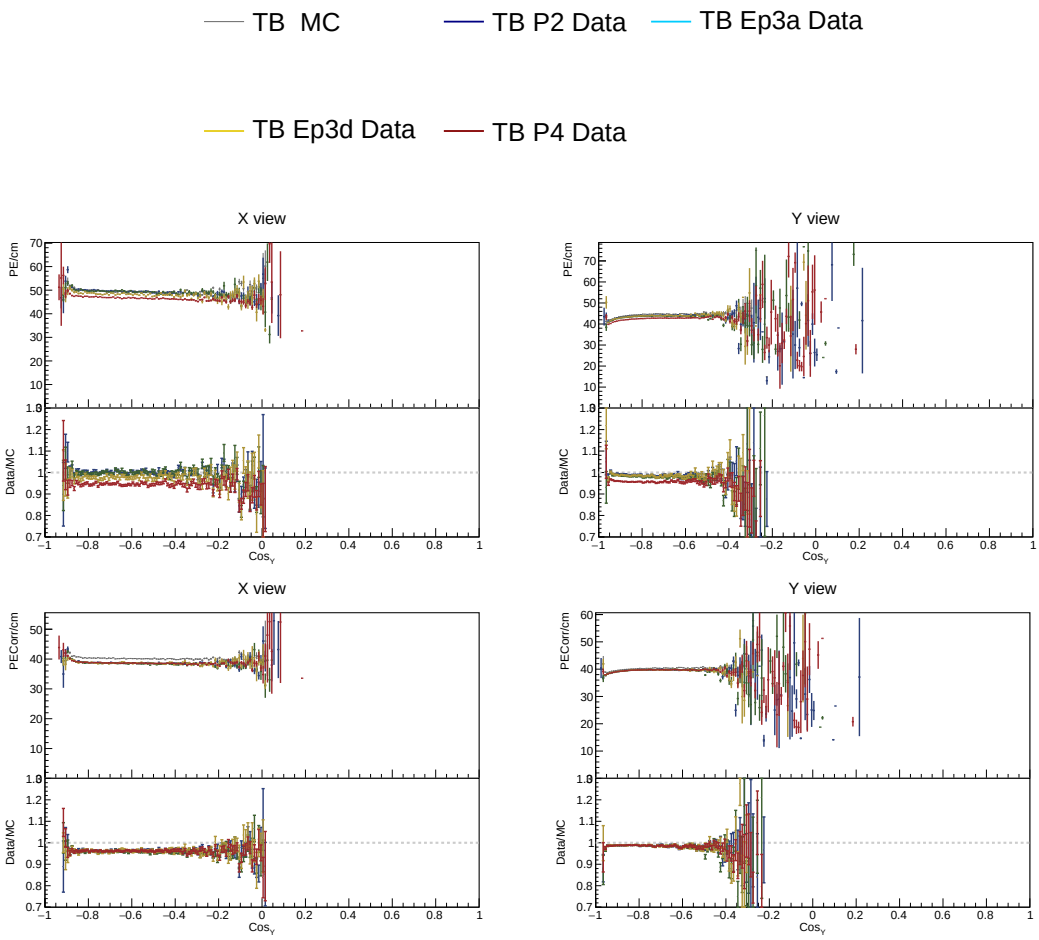

Figure A.9: Distributions of stopping muons within a 1-2 m track window from the end of their tracks across the cosine of the track angle from the Y (vertical) axis.

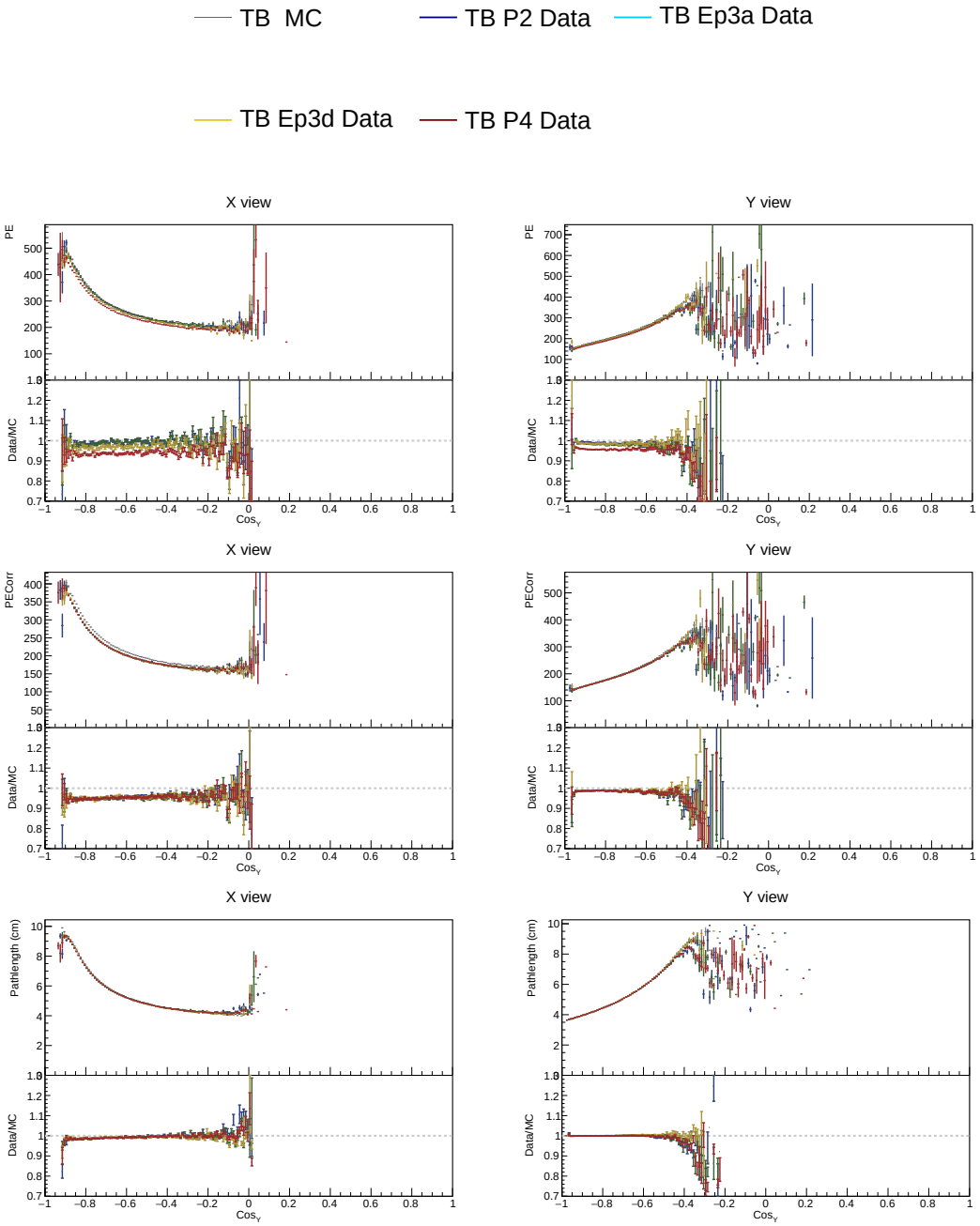

Figure A.10: Distributions of stopping muons within a 1-2 m track window from the end of their tracks across the cosine of the track angle from the Y (vertical) axis.

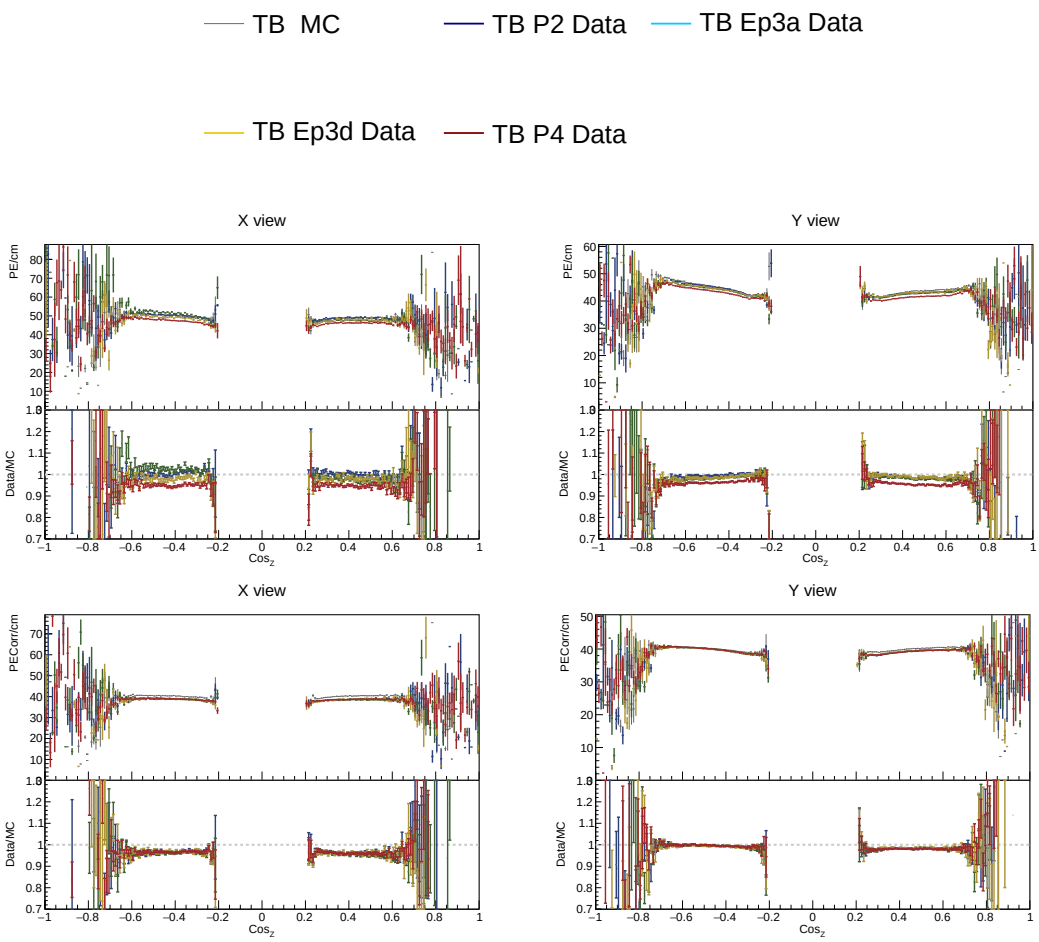

Figure A.11: Distributions of stopping muons within a 1-2 m track window from the end of their tracks across the cosine of the track angle from the Z (beam) axis.

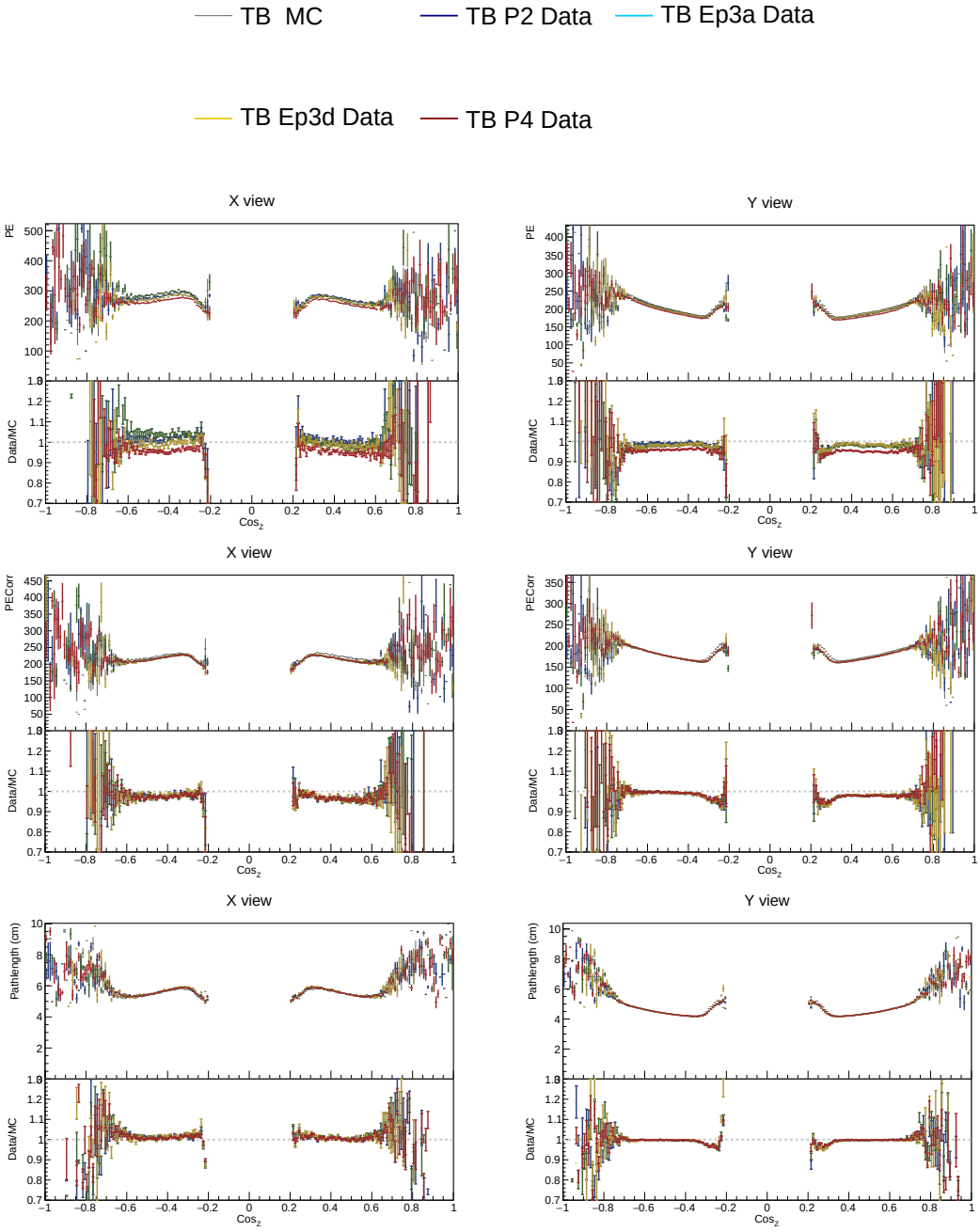

Figure A.12: Distributions of stopping muons within a 1-2 m track window from the end of their tracks across the cosine of the track angle from the Z (beam) axis.

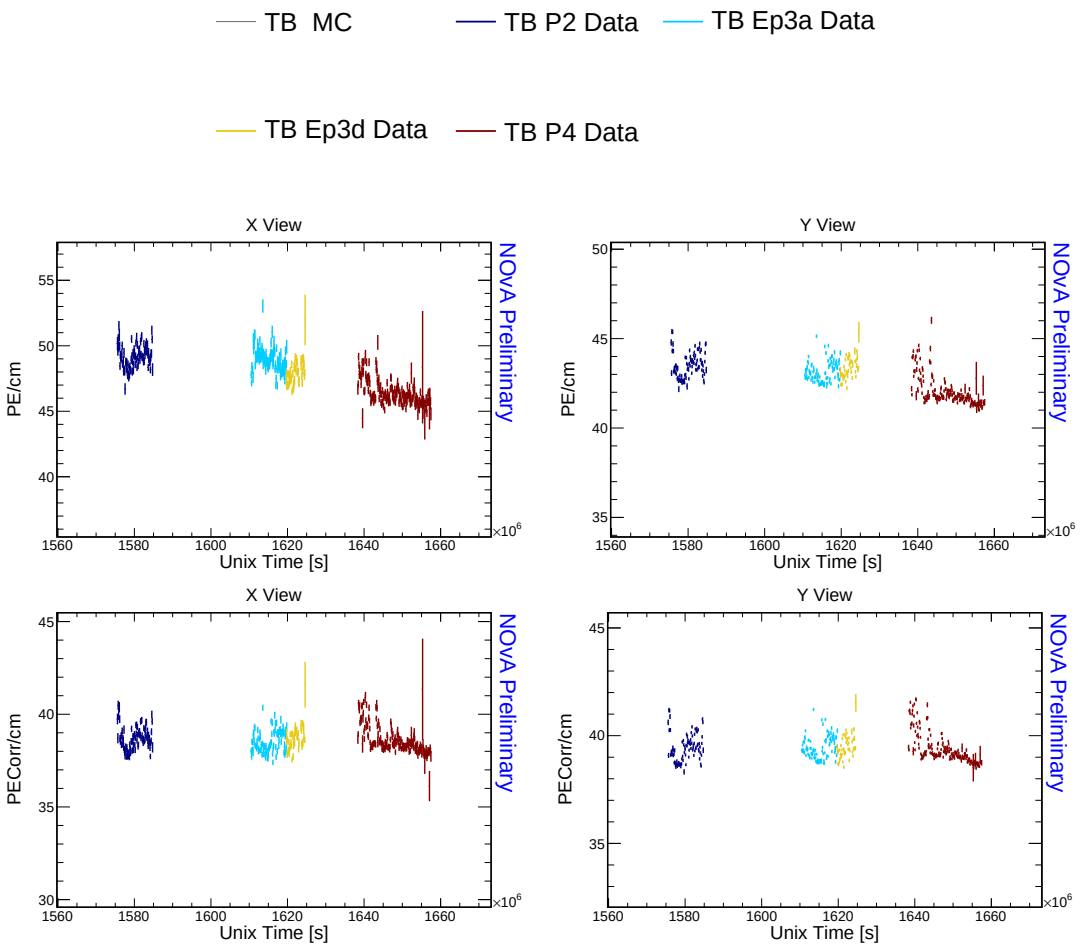

Figure A.13: Distributions of stopping muons within a 1-2 m track window from the end of their tracks across the event UNIX time.

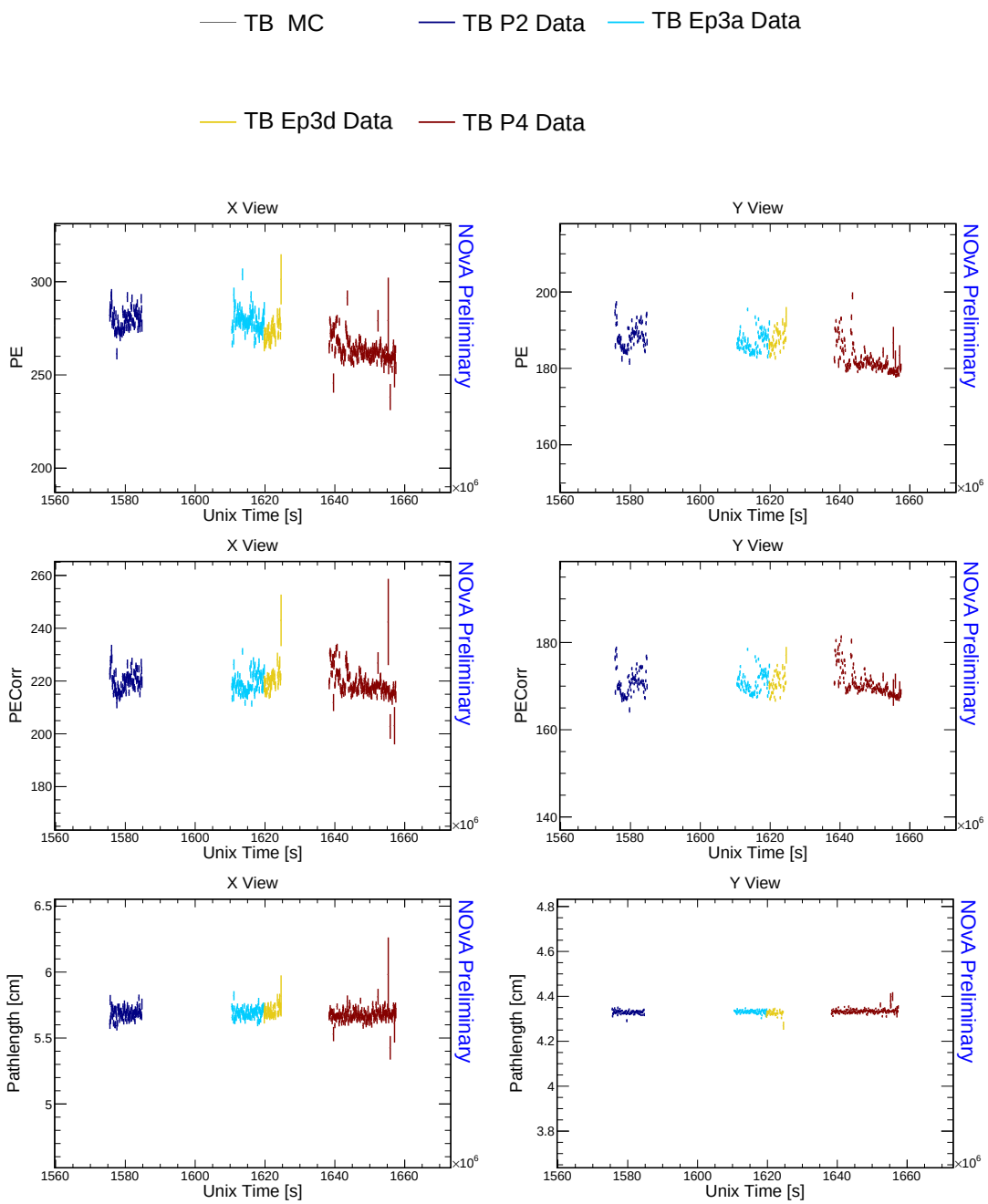

Figure A.14: Distributions of stopping muons within a 1-2 m track window from the end of their tracks across the event UNIX time.

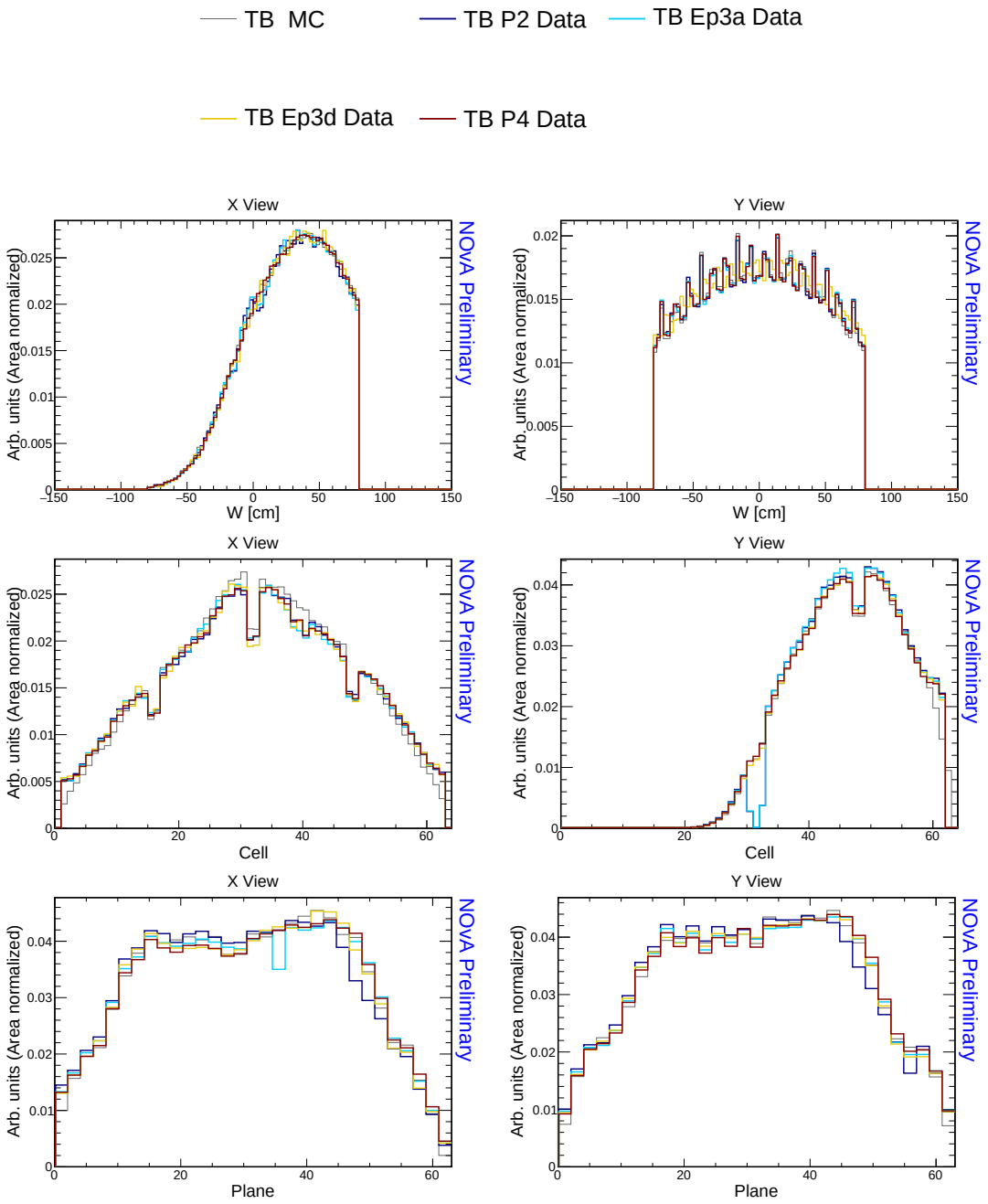

Figure A.15: Distributions of stopping muons within a 1-2 m track window from the end of their tracks.